THE CROWN ESTATE

Marine Estate Research Report

Wider implications of Macroalgal cultivation

ISBN: 978-1-906410-38-4

Published by The Crown

This report is available on The Crown Estate website at www.thecrownestate.co.uk

Dissemination Statement

Disclaimer

Suggested Citation

Aldridge, J., van de Molen, J. and Forster, R. 2012. 'Wider ecological implications of Macroalgae culitvation' The Crown Estate, 95 pages. ISBN: 978-1-906410-38-4

Cefas Document Control

Title: Wider ecological implications of macroalgal cultivation: final report

Submitted to:	Mike Cowling & Alex Adrian (The Crown Estate)
Date submitted:	26th October 2012
Project Manager:	Sonia Kirby
Report compiled by:	John Aldridge, Johan van der Molen, Rodney Forster
Quality control by:	Siân Limpenny
Approved by & date:	Stuart Rogers
Version:	7

Version Control History			
Author	**Date**	**Comment**	**Version**
J. Aldridge/J. Van der Molen/R.M. Forster	11/06/2012	Internal project team review	v 1
J. Aldridge/J. Van der Molen/R.M. Forster	25/06/2012	SR review	v 2
J. Aldridge/J. Van der Molen/R.M. Forster	26/06/2012	SL review	v 3
J. Aldridge/J. Van der Molen/R.M. Forster	29/06/2012	SR approval	v 4
J. Aldridge/J. Van der Molen/R.M. Forster	29/06/2012	Final Draft	v5
R.M. Forster	22/10/2012	RF/SL review	v6
S. Limpenny	22/10/2012	Final	v7

Wider ecological implications of macroalgal cultivation: final report

Authors: John Aldridge, Johan van der Molen, Rodney Forster

Issue date: 26th October 2012

Commissioned by: The Crown Estate

Head office

Centre for Environment, Fisheries & Aquaculture Science

Pakefield Road, Lowestoft, Suffolk NR33 0HT, UK

Tel +44 (0) 1502 56 2244 Fax +44 (0) 1502 51 3865

www.cefas.co.uk

Cefas is an executive agency of Defra

Table of contents

Executive Summary

The Crown Estate has begun to investigate the potential for large-scale production of macroalgae. One of the key issues that needs to be addressed before this becomes a reality is to assess the potential for wider ecosystem effects as a result of large-scale extraction of seaweeds. This is because the areas of greatest potential for farming seaweeds are likely to be located off Scotland's western coastline and island groups where the marine environment is relatively pristine. It is therefore sensible to explore the opportunities for farming macroalgae as a source of energy and determine the consequences for the wider marine environment.

This research project is aimed at addressing the potential effects of large-scale seaweed farming by using ecosystem modelling techniques. This will provide The Crown Estate with a strong evidence-base to determine the tradeoffs/interactions associated with large-scale macroalgae production versus protecting, conserving and enhancing biodiversity. In particular, the aim is to understand the effects of large-scale seaweed farming, with total yields perhaps in excess of one million tonnes per year, on the surrounding marine environment.

Two model approaches were used to assess the potential environmental impact of hypothetical macroalgae farms: a Combined Kelp Phytoplankton (CKP) compartment model simulating sites along the west coast of Scotland and a 3-D coupled hydrodynamics-biogeochemistry model simulating sites along the east coast of Scotland. The CKP model was developed to include a macroalgae growth model, whereas the 3D model was fitted with a nutrient sink to simulate the presence of a macroalgae farm.

The results of the CKP model in which the nutrient uptake of an algal farm was compared with a control (no farm) suggested very high impacts on phytoplankton biomass in the vicinity of the production area. The reduction in chlorophyll concentration as compared to the control decreased at larger scales, but was still greater than 10% at distances in excess of 7.5 km from the edge of the production area. This reduction in primary production will result in a local reduction in the biomass of herbivorous consumers such as zooplankton and filter-feeding benthic animals. A by-product of kelp farming is the release of large quantities of dissolved organic matter as well as continuously shedding fragments of blade material, particularly during the summer. Local deposition of this

material near the seabed in a stratified water column will provide opportunistic detritivores and omnivorous animals with a food supply, but will also cause enhanced respiration and locally reduce the oxygen concentrations. As with salmon farming, site placement is therefore very important to maximise kelp yields and to dilute waste products

The 3-D model results indicated potential reductions in annual-averaged, depth-integrated nutrient concentrations, production and biomass in a strip along the UK east coast from Stonehaven south, off the east coast of Scotland, to Norfolk. The magnitude of the changes depended on the model variable and on the intensity of the nutrient extraction (farming) imposed, varying from a decrease of over 40% for the most sensitive variables for the highest intensity farming scenario to less than a few percent reduction for non-sensitive variables and/or low-intensity farming. The far-field effects were not sensitive to the along-shore position of the farm, suggesting a more or less linear cumulative effect in the case of multiple farms. Lookup graphs and tables were constructed showing the extent of the area affected by a certain level of change as a function of the nutrient extraction intensity. These might be used to provide a first estimate of potential impact of macroalgae farms in similar settings/conditions.

The impacts simulated with the compartment model were smaller both in magnitude and in terms of the size and shape of the area affected than those simulated with the 3D model for equivalent farming intensity. These differences can be traced back to the assumptions made to set up the respective models. Comparison with field data from an experimental farm suggested that the magnitude was probably more accurately predicted by the compartment model, but the shape of the spatial extent of the impact was more accurately predicted by the 3D model. Therefore we expect the results for the lowest-intensity farming scenarios of the 3D model to be most representative of the potential impact of farming activity of the type proposed. The nitrogen removal associated with seaweed farming may be seen as beneficial in sea areas subject to high loading with anthropogenic nutrients, as this will reverse the eutrophication process. The annual inputs of nitrogen from sources such as the River Clyde or salmon aquaculture are however large (10000-20000 and 7500 tonnes N yr^{-1} respectively) compared to the 480 tonnes N yr^{-1} uptake capacity of the 20 km^2 kelp farm targeted in our compartment modelling. A farm of this size would remove a broadly similar amount of nitrogen to the 825 tonnes of N

currently removed to land each year by the main *Nephrops* fishery of the Malin Sea and Minches.

We conclude that the effects of the proposed farming activity on nutrient concentrations are expected to be 'marginally significant'. Given a sufficiently high level of farming activity (combination of intensity and size of the farm(s)), the effects might become 'certainly significant'. Definitions of these significance levels are provided in the report. The observable effects of nutrient removal would be a lower nutrient concentration in the water, decreased productivity and energy fluxes through the pelagic system, decreased flux of organic material to the seabed, and subtle alteration to community structure. These changes would occur in the long term against a background of considerable natural variability, and would require a dedicated monitoring programme to detect effects.

1 Introduction

Algae are regarded as a promising source of natural energy-rich material to supplement fossil fuels (Box 1). The Crown Estate have begun to investigate the potential for mass production of macroalgae (Kelly and Dworjanyn, 2008). One of the key issues that needs to be addressed before mass production of macroalgae becomes a reality is the potential for wider ecosystem effects as production is scaled-up. This is because the areas of greatest potential for farming seaweeds are likely to be located off Scotland's western coastline and island groups where the marine environment is relatively pristine. It is therefore sensible to explore the opportunities which exist around macroalgae as a source of energy to heat our homes and fuel vehicles and determine the consequences for the wider marine environment.

In 2011, The Crown Estate and Cefas initiated the present project to investigate some of the environmental issues which might occur if the cultivation of seaweeds around Scotland were to be increased. The project brief was primarily to assess the impact of an algal farm of size 1000-2000 hectares (10—20 km^2) on the local and regional patterns of nutrient concentration, and to consider any other biogeochemical impacts associated with seaweed production. The primary ecosystem impact to be investigated was "does any depletion of nutrients occur outside of the seaweed farm, and are these effects significant?" Additional questions concerned the impact of organic materials and volatile gases released by an actively-growing kelp production unit.

A premise of The Crown Estate was that a Scottish cultivation system could produce in the order of 20 tonnes of dry seaweed per hectare per growth season, based on research in the Netherlands (Reith, 2009 – presentation to Seaweed Bioenergy Research Forum). The growth rates of macroalgae are certainly sufficient to produce such a yield, in fact quantities of close to 50 tonnes ha^{-1} yr^{-1} can be produced in aerated tank systems (Lüning and Pang 2003). Floating raft systems are used in China to grow the kelp *Laminaria* for human consumption. The northern Huanghai Sea supports up a harvest of up to 18 tons of dry kelp per hectare, with lower yields in the south of 13-15 tons due to a shorter growing season. Fertiliser contained in clay pots attached to the seaweed farms is used in Chinese mariculture to support high yields in some offshore areas where nutrients are naturally low.

Densely-packed natural stands of macroalgae and seagrasses can fix carbon at rates similar to the most productive terrestrial systems, with an upper limit of close to 2 kg C m^{-2} yr^{-1} (Lüning 1990). The expected yield of 20 tonnes dry weight ha^{-1} yr^{-1} equates to a net primary production of 0.6 kg C m^{-2} yr^{-1}, thus well within the range of possibility. Dring (2012) described the yield of a net-based open water cultivation of the red macroalgae *Palmaria palmata* as being 10 kg wet weight per m^{-2} yr^{-1} which equates to 0.4 kg C m^{-2} yr^{-1}. Such a level of production would however be 3 to 6 times higher than the typical net productivities of phytoplankton-based systems around the UK.

Box 1: Algae as an energy source

The mass production of algal biomass, and conversion of this material into high-calorific fuel for energy production has been listed as one of the 'five technologies that can change everything' (*Wall Street Journal: Energy*, 19th October 2009; **http://tinyurl.com/yfwo33a**). In the UK, the Department of Energy and Climate Change has identified different pathways that energy production and demand might follow, using an interactive tool which allows the user to assess different future scenarios between now and 2050. The cultivation of marine seaweeds is identified by DECC as a possible future source of low-carbon energy. Different scales of seaweed production are envisaged: level 1 of the Carbon Calculator tool assumes that an area of 560 km^2 of sea surface could produce up to 4 Terawatt hours of energy per year, and would be equivalent in scale to half of the natural production of seaweeds around Scotland, whereas an algal farm scaled-up to level 4 would cover 4700 km^2 and would generate 46 TW h yr^{-1}. For comparison, a small nuclear plant such as Sizewell B in Suffolk produced 4.7 TW h yr^{-1} in 2010, and wind power generated 9.1 TW h^{-1} in 2009.

Marine macroalgae are at present thought more amenable to cultivation than microalgae (phytoplankton): there is a long history of natural harvest of seaweeds on the western coasts, as well as a recent history of small-scale seaweed farming. Other European countries have far greater exploitation of their natural seaweed resources than the U.K. Norway harvests annually around 150000 tonnes wet weight of kelp (*Laminaria* species, mainly *L. hyperborea*) for alginate production. The Norwegian standing stock of kelp is

estimated to be 50-100 million tonnes (Steen 2009). An estimate of kelp biomass for the coastal waters around Scotland was made by Walker (1954). A combination of detailed ship surveys and aerial reconnaissance were used to estimate a total of 3-4 million imperial tons of *Laminaria* resource at that period of time.

In this report, the nutrient requirements of a 1000-2000 hectare seaweed farm are compared to the availability of naturally available dissolved nutrients for different locations on the Scottish west coast. The harvesting of seaweed crops for use in energy production results in a net removal of nutrients from the sea to the land, which could potentially lower the productivity of the marine system. The nutrient withdrawal by seaweed could counter-balance inputs of nutrients to the coastal zone by aquaculture. From a global nutrient management perspective, overcoming the effects of increasing nutrient release from finfish and shellfish production could be achieved with integrated systems that include seaweed farms to reduce excessive nutrient loading (Bouwman et al. 2012).

The report discusses nutrient removal by seaweed farming in relation to other sources and sinks of nutrients on the Scottish west coast, some of which are far greater in magnitude. These include natural sources and sinks of nutrients as well as anthropogenic sources such as aquaculture and urban or agricultural discharges.

This is the final report of the project and describes the results of the application of two different models for assessing potential wider scale impacts of large scale growth of macroalgae. An intermediate report was submitted (Cefas 2012) which described in detail the physiological characteristics of three kelp species which were considered at the outset as potential candidates for kelp farming. The growth and nutrient storage characteristics were used to parameterise the models where possible. A description of the prevailing oceanographic and meteorological conditions at sites around the west coast of Scotland was also presented in Cefas (2012), and used as forcing conditions for model runs.

2 Methods

2.1 Seaweed farming: crop yields, nutrient removal to land and modelling requirements

An example of yields achievable in a small-scale algal cultivation system is described by Peteiro et al. (2010) for a kelp farm (using the species *Undaria*) located in the upwelling region of Galicia in Spain. The farm consisted of vertical ropes seeded with small thalli in the early Spring, then transplanted to the sea at intervals of 2 m along horizontal lines set 4 m apart. At harvest, after 130 days of growth in the sea, each vertical rope was densely packed with *Undaria* plants. The average frond length was 120 cm with a mean wet weight of 260 g per thallus. A metre of vertical rope produced almost 10 kg of wet weight. Assuming rope lengths of 3 m then on an areal basis the system produced 3.6 kg wet weight m^{-2} in four months at sea (equivalent to 163 g C m^{-2} yr^{-1}, assuming only 1 harvest). Thus, this was a moderately productive farm with yields similar to or slightly higher than natural kelp populations, but lower than that of the most productive seaweed cultivation areas in China.

The first consideration for assessing the environmental impacts of algal farming in the open sea is to examine the nutrient requirements of the farmed species with respect to the natural supply of dissolved inorganic nutrients (nitrates, phosphates). This calculation can be done in a rather simple manner for the moderately-productive *Undaria* farm described above. The harvest of 163 g C m^{-2} in the algal blades is accompanied by the removal to land of a lesser amount of nitrogen, approximately 11 g N m^{-2} in accordance with a mean C:N ratio of 15 for kelps (Broch & Slagstad 2011). The nitrogen required to support the kelp harvest is 0.8 mol N m^{-2}, and the nitrogen available in the water column is approximately 0.2 mol N m^{-2}, assuming a fully-mixed water column with a depth of 50 m and a mean annual concentration of 4 µM N. Thus, this type of kelp farming would fully remove nitrogenous nutrients from a sea area four times larger than the farm itself. A higher intensity of kelp production would remove proportionately more nutrients from the surrounding seawater. In reality, nutrients are available at different concentrations at different times of year, are transported through the farm with the currents and tides, and in an open system macroalgae must compete for nutrients for phytoplankton. Hence, a

modelling approach is needed to calculate the true impact of an algal farm on its environment.

Two different models were used: firstly - a compartment or box model with realistic simulation of kelp physiology, light requirements, nutrient uptake and storage, and interaction with phytoplankton. From this model, calculations were made of the spatial extent of nutrient removal and potential losses to planktonic productivity in the surrounding area. The calculated production of kelp biomass was also used to infer the effects of cast-off algal blades and extracellular organic material on oxygen consumption in the surrounding environment. Secondly – a coupled hydrodynamic-biogeochemical model of the North Sea was used to assess the regional scale ecosystem response to nutrient removal from a model grid cell representing a large kelp production area.

2.2 Compartment modelling

The dynamic Combined Phytoplankton Macroalgae (CPM) model (Aldridge et al. 2010) was used as the basis to develop the Combined Kelp Phytoplankton (CKP) model used in this study. The CKP model simulates seasonal cycles of phytoplankton, nutrient (as nitrate) concentration and macroalgae biomass taking account of the dynamic partitioning of available nutrients between phytoplankton and the macroalgae. For this project the original CPM model was extended to: 1) include the physiology of kelp-like macroalgae; 2) include a simple transport capability so that far-field as well as local effects could be assessed.

Attention was focussed on modelling the kelp species *Saccharina latissima* (formally known as *Laminaria saccharina*). Other species of interest (*Laminaria hyperborea*, *Laminaria digitata*) showed similar although not identical behaviour (Cefas 2012), particularly during the first year of growth. However we believe that the model results obtained from the example of *Saccharina latissima* are sufficient to indicate the main wider impacts of large scale kelp cultivation on the broader ecosystem.

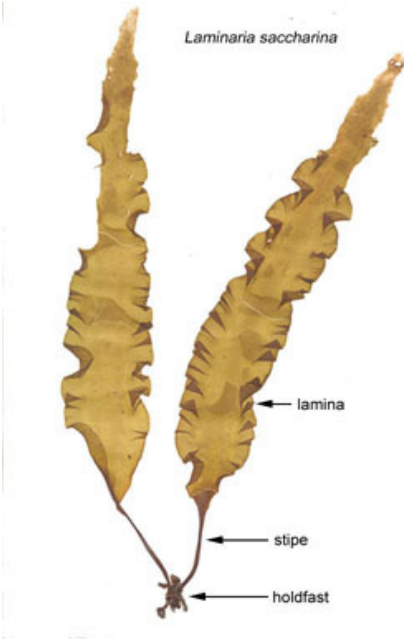

Figure 1: Structure of *S. latissima*, from http://www.ohio.edu/plantbio/vislab/algaeimage/pages/laminaria.html

Transport processes in the CKP are modelled by defining a number of linked well-mixed water bodies that exchange phytoplankton and nutrients across their boundaries. Within a given compartment the functional structure of the model is as shown in Figure 2. A full description of the model formulation and calibration is given in Appendix A. The macroalgal sub-model of the CKP predicts the lamina[1] projected area (Figure 1) and the internal nitrate and carbon content of the lamina. The stipe and holdfast are assumed to play a minor role in the nutrient demand of the plant.

[1] The term lamina, frond or blade refer to the same portion of the plant (Figure 1) and are used interchangeably in the text.

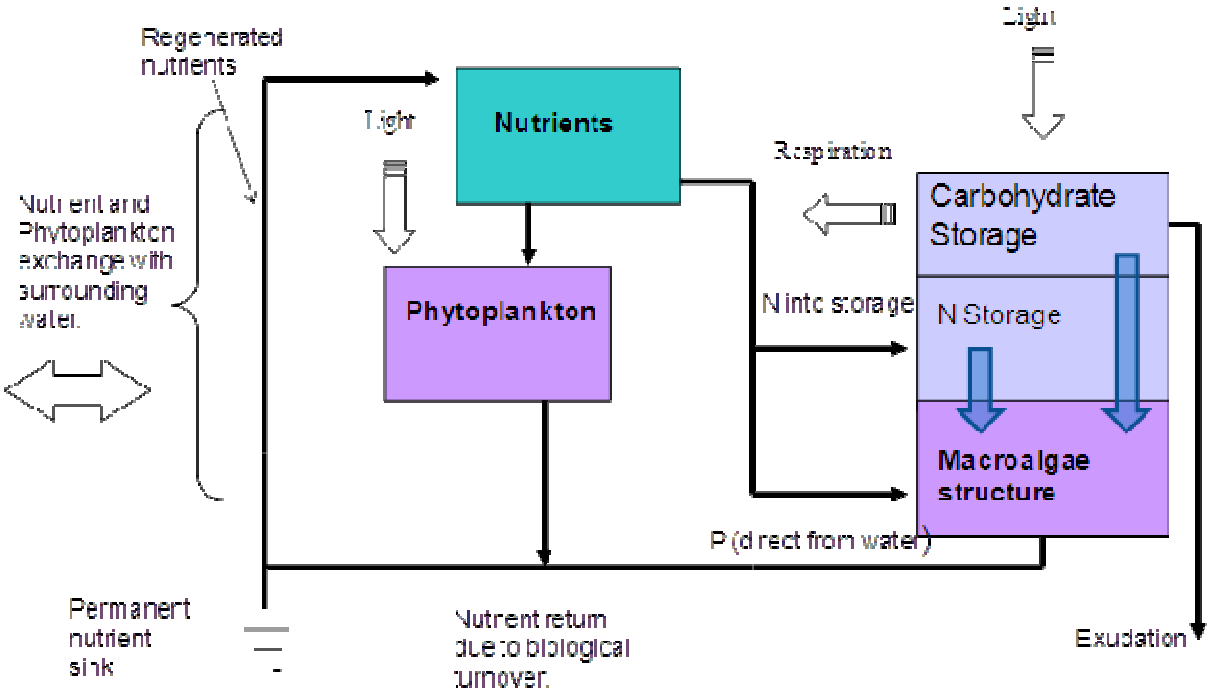

Figure 2: High level schematic of modelled processes in the CKP model.

Due to the relatively simple nature of the physical transport mechanism implemented, the model cannot make highly site specific predictions but can be used to explore the envelope of possible impacts of a generic site. Full site specific capability would require coupling to a 3D hydrodynamic model of the particular site which was beyond the scope of this study.

2.2.1 Compartment model Scenario setups

The Crown Estate suggested several areas of interest at the onset of the project for which kelp modelling should be done: these areas were distributed along the west coast of Scotland. Descriptions of the environmental conditions at these locations were given in Cefas (2012) following a literature review. In summary, the Scottish Coastal Current (SCC) transports water northwards along the west coast of Scotland (Turrell et al. 1996; Figure 3a). The origin of this water is the Irish Sea via the North Channel, and the SCC is distinguished from offshore Atlantic water by its slightly lower salinity. North of the

Minches, the SCC merges with an eastward flowing slope current and becomes part of the Fair Isle Current to the west of Orkney, continuing eastward to enter the North Sea. Inflowing Atlantic waters with high salinity travel south along the east coast of Scotland and form an important part of the total nutrient supply to the North Sea (Holt et al. 2012).

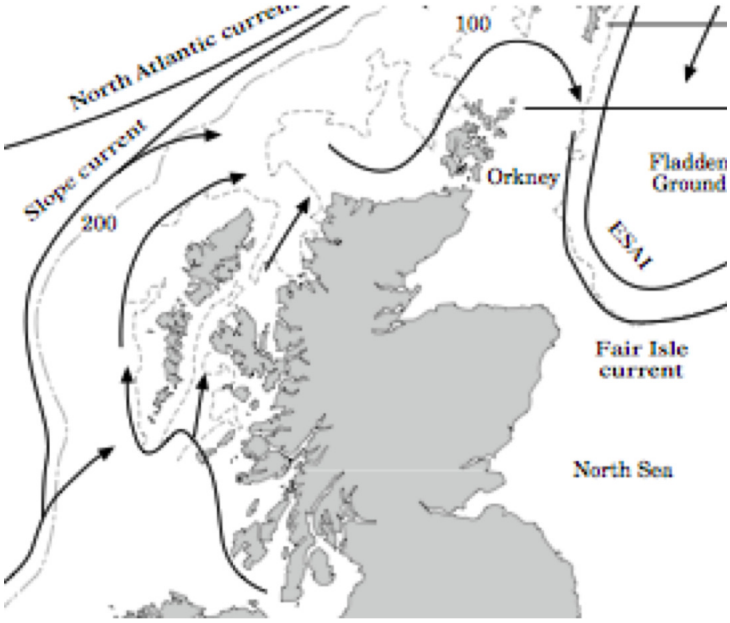

Figure 3a: General description of ocean currents around the Scottish coast (from Turrell et al. 1996).

The Scottish western coastal sea, to the extent of the 12 mile limit, covers an area of approximately 50000 km^2 (Scotland's Marine Atlas 2011). At the beginning of the spring growth season, when nutrient concentrations are at their highest, this sea area contains in the order of 350 000 tonnes of dissolved inorganic nitrogen. Throughout the year there are additional inputs of nitrogen to the sea from the atmosphere and the land. The contribution from the atmosphere is small, of the order of 15000 tonnes N per year, whereas land sources add 120000 to 150000 tonnes of N each year. This mix of dissolved inorganic and organic forms of nitrogen plus some particulates arrives from rivers, urban waste and industry, and aquaculture (Heath et al. 2002; Rydberg et al. 2003). The nutrient load is not divided evenly by rivers around the coast of Scotland, with highest inputs on the

south-west (Clyde area) and east coasts (Firth of Forth), and very low inputs to the north-west region despite heaviest rainfall and a strong river run-off.

Four sites identified for modelling assessment (Figure 3b) were clustered into two generic model setups based on their nutrient and optical characteristics. Sites 2,3,4 (offshore Mull, Tiree and Ullapool) appear to have broadly similar nutrient and light attenuation conditions with winter nitrate concentrations of 5-7 mmol m^{-3} and light attenuation coefficients of the order K_d=0.2 m^{-1}, (Cefas 2012). For the purpose of modelling these sites are treated as equivalent with a generic model set up. Nutrient conditions at site 1 (Clyde Sea) are higher than that of the other locations, with winter nitrate concentrations of around 10 mmol m^{-3} (Slesser & Turrell 2005). A satellite-based estimate of underwater light attenuation at site 1 was higher (K_d=0.3 m^{-1}) than at the other locations. Because of these differences site 1 was modelled separately from sites 2,3 and 4.

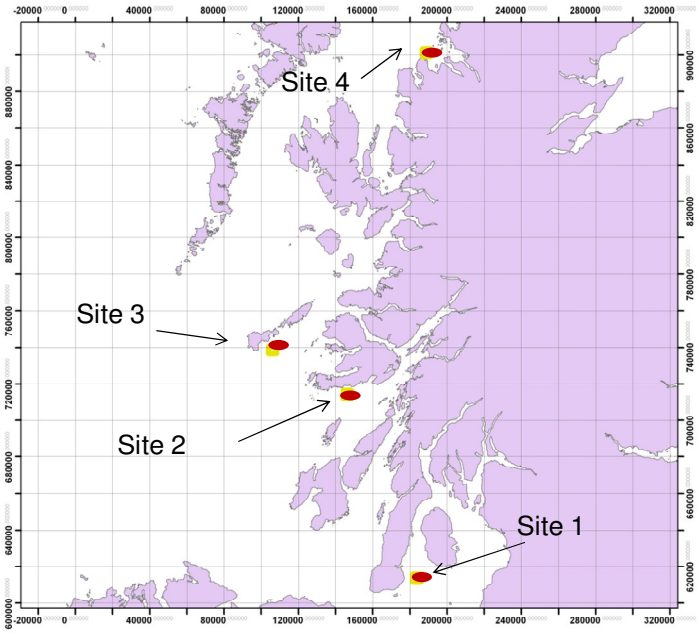

Figure 3b: Example sites for model scenarios.

The compartment model was setup to represent the nested configuration shown in Figure 4 with an inner region of diameter 5 km enclosed within a 10 km middle compartment and a 20 km outer compartment. Average water depths are specified for each

compartment. This simple compartment modelling approach cannot represent the actual coastline, water depth distribution or the tidal dynamics of the flow. Hydrodynamic transport processes are represented via exchange of nutrients and phytoplankton, which occur between adjacent compartments based on a user-specified water volume flux. The outermost compartment exchanges nutrients and phytoplankton with the surrounding sea environment via a set of specified time varying boundary concentrations described in Cefas (2012).

The inner region (area 20 km^2) is assumed to represent the macroalgal production area. No macroalgae are allowed to grow in the surrounding compartments. The inner compartment size was set based on a tidal excursion for a relatively weak tidal flow (peak speed 0.35 m s^{-1}) but also represents approximately the upper size of the proposed large scale macroalgal production area. It should be noted that although the plot shows a circular arrangement the model itself is not spatial, and calculations are made on the total areas without regard to the shape of the region. In reality, the transport of material will have a directional component determined by the residual flows in the region and impacts will be greater at locations aligned with the preferred transport direction. Thus the nominal distances represented by the compartment diameters (Figure 4) are a minimum distance of impact assuming dispersion equally in all directions. That is, a predicted effect in the outer compartment shown (nominally representing a distance 7.5 km from the edge of the production area) should be interpreted as being the minimum distance for this level of impact.

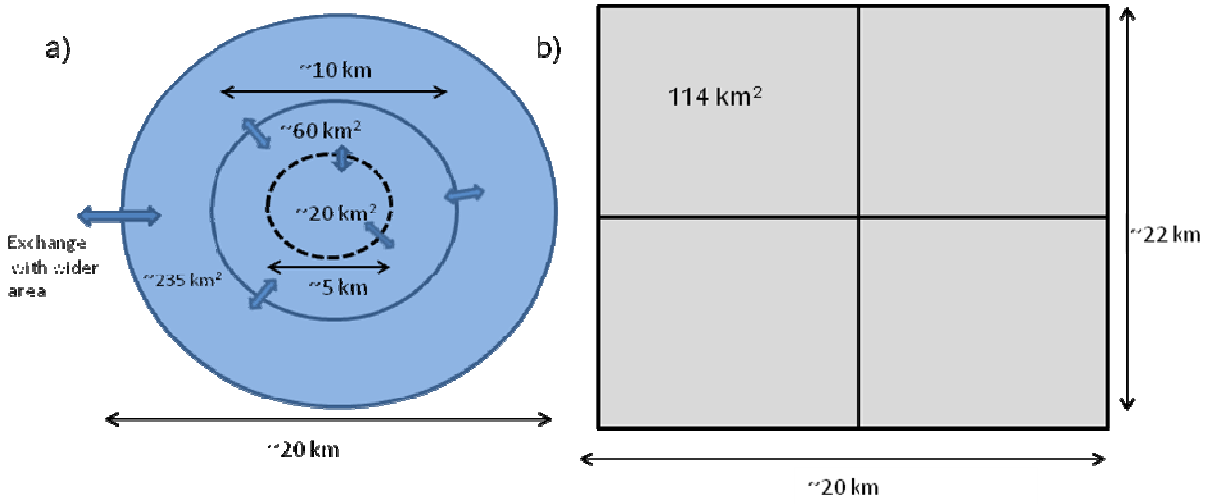

Figure 4: Schematic of the spatial configuration. a) 'Inner', 'Middle' and 'Outer' Compartments of the Combined Kelp Phytoplankton model in comparison with b) approximate relative scale of 2 x 2 grid of GETM-ERSEM boxes. One grid cell of the ERSEM was converted into a nutrient sink.

In addition to the nested arrangement, a single region of 20 km diameter was set up for the two generic sites. This single equivalent region was used to calculate an exterior boundary condition for the nested region and also to provide reference condition with no macroalgae present to compare against simulations with macroalgae.

The water column in both the Clyde Sea and western Scottish coast is generally stratified, both thermally in summer and by salinity differences due to freshwater runoff. Stratification isolates the less-dense upper layer of the water column from colder nutrient-rich bottom water, and will limit access to nutrients for plants growing in the surface layer. The appropriate water depth to use is not the entire water column but that of the upper mixed layer. Based on sections of temperature salinity and nutrients for the Minch shown in Gillibrand et al. (2003) a value of 15 m was taken for this depth in the model for sites 2, 3 and 4. The available nutrient pool was drawn down to this depth only, with no mixing assumed to occur with deeper waters. Similarly measurements in the Arran Deep in the Clyde Sea in February and July (Matthews et al., 1999) suggest values between 10 and 20 m for the mixed layer depth when stratification is present. A value of 15 m for the water depth was therefore also used for simulations at site 1. Macroalgae were assumed to lie at approximately 1.5 m below the water surface.

The volume exchange between compartments was calculated as the product of the common cross sectional area joining the regions and a 'mixing velocity'. The mixing velocity was assumed uniform for a given site and set to produce 'reasonable' flushing times between the compartments in Table 1. The flushing time is here defined as the time taken for half the volume to be exchanged with the surrounding region. This type of formulation is suitable for modelling over time scales larger than a tidal period and describes the changes in concentrations as impacts are diluted within larger volumes of water.

Light availability for macroalgae was calculated based on latitude, water depth and light attenuation. Since the main aim of this study was to investigate environmental consequences of macroalgal production rather than the optimal conditions for macroalgal growth, factors such as self shading at high macroalgal densities were not considered. Thus it is assumed that high densities can be achieved without light limitation occurring. At the very high densities envisaged for large-scale production however, this may be an important consideration.

Common Parameters	**Outer**	**middle**	**Inner**	**Notes**
Area	235 km^2	60 km^2	20 km^2	Based on circular compartments
Depth **Light attenuation coefficient**	15m Site 1 0.3 m^{-1} Site 2,3,4 0.2 m^{-1}	15m Site 1 0.3 m^{-1} Site 2,3,4 0.2 m^{-1}	15m Site 1 0.3 m^{-1} Site 2,3,4 0.2 m^{-1}	Upper layer Cefas (2012)
Exchange rate with surrounding compartment	0.048 d^{-1} (flushing time 14 days)	0.092 d^{-1} (residence half life 7 days)	0.138 d^{-1} (residence half life 5 days)	Based on cross section area and assumed mixing velocity of 0.002 ms^{-1}
Site 1 specific peak winter nitrate	10 mmol m^{-3}	10 mmol m^{-3}	10 mmol m^{-3}	Rippeth and Jones (1997)
Site 2,3,4 specific peak winter nitrate	7 mmol m^{-3}	7 mmol m^{-3}	7 mmol m^{-3}	Slesser and Turrel (2005)

Table 1: Compartment model run parameters.

Target peak macroalgal yields of around 20 tonnes dry weight per hectare were assumed (equivalent to approximately 1000 $dm^2\ m^{-2}$ in terms of frond area per sea surface area, or a Leaf Area Index of 10). The frond area density of plants specified at the start of the model run (termed A_0 with units $dm^2\ m^{-2}$) is important in determining the peak biomass achieved and in the simulations the value of A_0 was adjusted to yield approximately the target peak biomass at site 1 (Clyde Sea). The same value of A_0 was then used for the other

generic west coast site to see if the same yield could be obtained at locations with lower nutrient concentrations. The value of A_0 also acted as a minimum area density with macroalgal density not allowed to decrease below this value, on the assumption that over a complete growing season there would be no net decrease in the amount of macroalgae.

The exchange rate between compartments is user specified as it is important to assess the sensitivity of model results to the exchange rate. Therefore in separate runs the exchange rates were uniformly scaled down by 0.5 to obtain a low flushing rate situation and up by 1.5 to yield a higher flushing rate situation and the change in annual mean and peak phytoplankton and nitrate concentrations were noted. Changes in nutrients and phytoplankton are presented relative to reference runs with the same exchange rates but no macroalgal present. The effect on phytoplankton growth of reduced light levels due to the presence of macroalgae cover was also investigated in an additional model scenario whereby the light available to phytoplankton was reduced close to zero in the inner compartment.

The kelps in general exhibit high loss rates of organic carbon fixed during photosynthesis. This may be an adaptive response to maintain a smooth blade surface and prevent biofouling, whereby regular sloughing of the surface layer can reduce drag. Additionally, algae may operate a form of overflow metabolism when light levels and carbon fixation rates are high but nutrients are limiting to growth. Experimental observations indicate that 20-60% of gross primary production may be lost as exudates (Wada et al. 2007; Abdullah & Fredriksen 2004), and this loss term is included in the CKP. Fracture of the frond tips due to wave action and grazer-induced damage also releases particulate organic material to the water column. In extreme cases of storm damage whole plants or blades may be released and will accumulate on the seabed or be deposited on local intertidal areas. The fate of the organic material produced by kelps depends upon its composition. Low molecular weight carbohydrates will be rapidly assimilated by bacteria and planktonic eukaryotes, whereas long-chain or phenolic compounds are refractory and can persist in seawater for some time. Macroalgal exudates are thought to contribute significantly to the pool of chromophoric dissolved organic material (cDOM) in coastal waters (Hulatt et al

2009). Particulate fragments lost from natural kelp forests or kelp farms can be ingested directly by larger invertebrates, or will be gradually broken down to smaller particles and ultimately enter the dissolved fraction.

To consider the fate of kelp detritus, the biological oxygen demand associated with exudates and frond loss was also investigated. The CKM model provided an estimate of the grams of carbon per day released from the macroalgae. A worst case situation was assumed to occur in which all of the organic material shed by the kelp canopy sank to the bottom mixed layer (BML) of either the 'inner' area (e.g. material falling to the seabed immediately below the kelp farm) was dispersed across the seabed of the 'inner' plus 'middle' areas. As with the nutrient calculations, the flushing rate was altered to produce different scenarios. The biological oxygen demand was estimated assuming a complete utilisation of all carbon by the microbial community with a respiratory quotient of 1.0, and expressed as the change in oxygen saturation of the lower water column.

2.3 GETM-ERSEM-BFM modelling in 3D

A coupled physical-biogeochemical model was fitted with a nutrient sink to simulate the effects of macroalgae farms on the marine biogeochemical environment. Specifically, the model was applied to Scottish coastal waters in the North Sea as an initial demonstration of the potential spatial footprint of large-scale macroalgae farming.

2.3.1 Model description

The coupled physical-biogeochemical model GETM-ERSEM-BFM was used for the simulations. GETM (General Estuarine Transport Model) is a public domain, 3D Finite Difference hydrodynamic model (www.getm.eu). It solves the 3DV shallow-water equations and equations for conservation of salt and heat. The ERSEM-BFM (European Regional Seas Ecosystem Model - Biogeochemical Flux Model) version used here is a development of the model ERSEM III (see Baretta et al., 1995; Ruardij & van Raaphorst, 1995; Ruardij et al., 1997; Vichi et al., 2003; Vichi et al., 2004; Ruardij et al., 2005; Vichi et al., 2007; www.nioz.nl/northsea_model), and describes the dynamics of the biogeochemical fluxes

within the pelagic and benthic environment (Figure 5). It simulates the cycles of carbon, nitrogen, phosphorus, silicate and oxygen and allows for variable internal nutrient ratios inside organisms, based on external availability and physiological status. The model applies a functional group approach and contains four phytoplankton groups, four zooplankton groups and five benthic groups, the latter comprising four macrofauna and one meiofauna groups. Pelagic and benthic aerobic and anaerobic bacteria are also included. The pelagic module includes additional processes over the oceanic version presented by Vichi et al. (2007) to make it suitable for temperate shelf seas: (i) a parameterisation for diatoms allowing growth in spring, (ii) enhanced transparent extracellular polysaccharides (TEP) excretion by diatoms under nutrient stress, (iii) the associated formation of macro-aggregates consisting of TEP and diatoms, leading to enhanced sinking rates and to a sufficient food supply the benthic system especially in the deeper offshore areas (Engel, 2000), (iv) a Phaeocystis functional group for improved simulation of primary production in coastal areas (Peperzak et al., 1998), and (v) a suspended particulate matter (SPM) resuspension module that responds to surface waves for improved simulation of the under-water light climate. The ERSEM-BFM model used here also includes a 3-layer benthic module, which enables it to resolve substantially more benthic processes and more detailed benthic-pelagic coupling than other biogeochemical models recently applied to the North Sea (Radach & Moll, 2006; Lenhart et al., 2010), and making it suitable for the present study.

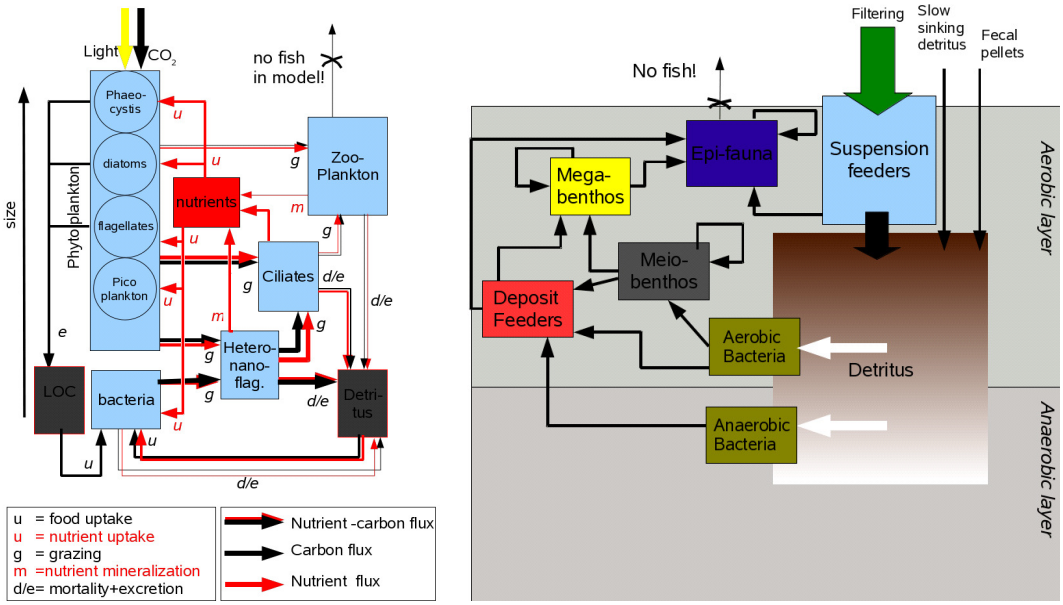

Figure 5. Schematic representation of the pelagic (left) and benthic (right) parts of the ERSEM-BFM ecosystem model.

2.3.2 Model validation

Regular validation of the model is carried out as part of the on-going model development using observations from the Dutch maritime area. Also, validation was carried out on areas in the central and southern North Sea as part of work carried out for OSPAR (Lenhart et al., 2010). For the purpose of the current work and report, additional validation was carried out through graphical comparison of nutrient concentrations with observations from the Stonehaven research station for which a long and detailed time series of oceanographic variables is available (see below for fuller description of site characteristics).

2.3.3 Nutrient sink to simulate macroalgae farms

Macroalgae farms have a number of potential impacts on the marine ecosystem, the most important of which are a) extraction of nutrients and carbon, b) shading, c) production of detritus (see CKP Model description and results). A simple nutrient sink was implemented to simulate the potential spatial impact of nutrient extraction (i.e. ignoring the influence of shading and detritus production). The nutrient sink was designed using characteristics of kelp nutrient uptake, based on the CKP Model (see Appendix B). It was assumed that the kelp farm covered one grid cell in the model (approx. 10.1x11.1 km) completely, and that it was active year-round. Simulating presence of macroalgae throughout the year was expected to result only in a slight overestimate when compared to having nutrient take-up in winter only, because nutrient concentrations are naturally low in summer through uptake by phytoplankton, and the nutrient uptake capacity of the seaweed in the model reduces during periods of low nutrient concentrations. The model was run for the years 1995-2008, considering 1995-2004 as spin-up[2] for the benthic system which has a long response time, for a reference scenario (no farms) and several macroalgae farm scenarios (Figure 6, Table 2).

[2] Running a model for a period of time to let it adjust to sudden changes such as initial conditions or artificial changes in setup or forcing; a spin-up period is usually discarded, and only model results obtained following that are considered.

Two locations off the Scottish East coast were considered: one coinciding with the Stonehaven research station, and one off Dunbar to the south of the Firth of Forth. The Stonehaven site is in waters essentially supplied by Atlantic nutrients (i.e. 'natural' nutrient concentrations), whereas the Dunbar site is in waters slightly enriched with anthropogenic nutrients in the plume of the Firth of Forth. For the Stonehaven site, four scenarios were considered with different farming intensity, and for the Dunbar site, two scenarios were run (Table 2).

A 1000 dm^2/m^2 areal coverage of one grid cell (10.1x11.1 km^2) in the model with macroalgae corresponds to 10 layers of blades covering the whole area of the grid cell. This density coincides with the desired production capacity per square metre. Results were annually averaged and depth-integrated, and the relative differences with the reference scenario were calculated. Subsequently, maps were produced of the relative differences in pelagic and benthic geochemical and primary and secondary biological variables[3], averaged over the years 2005-2008. Lookup-charts for the potential area impacted as a function of farming intensity were compiled from the model results for the Stonehaven site. These may be used to provide a first rough estimate of potential impact for projected farms in similar settings.

Scenario	**Description**	**Farm location**	**Coverage (A [dm^2/m^2])**
1	Stonehaven site	57N 2.15W	100
2	Stonehaven site	57N 2.15W	50
3	Dunbar	56N 2.32W	100
4	Stonehaven site	57N 2.15W	1000
5	Dunbar	56N 2.32W	1000
6	Stonehaven site	57N 2.15W	500

[3] Phosphate, nitrate, ammonium, silicate, chlorophyll, oxygen, CO2, pH, dissolved inorganic carbon,diatoms, flagellates, picophytoplankton, dinoflagellates, phaeocystis colonies, net primary production, gross primary production, TEP, particulate organic carbon,carnivorous mesozooplankton, omnivorous mesozooplankton, microzooplankton, heterotrophic nanoflagellates, gross secondary production, net secondary mesozooplankton production, net secondary microzooplankton production, faecel pellet particulate organic carbon, pelagic bacteria, epibenthos, deposit feeders, suspension feeders, meiobenthos, benthic predators, particulate organic carbon, oxygen penetration depth, denitrification layer depth, nitrate in sediments

Table 2. GETM-ERSEM-BFM model scenario runs

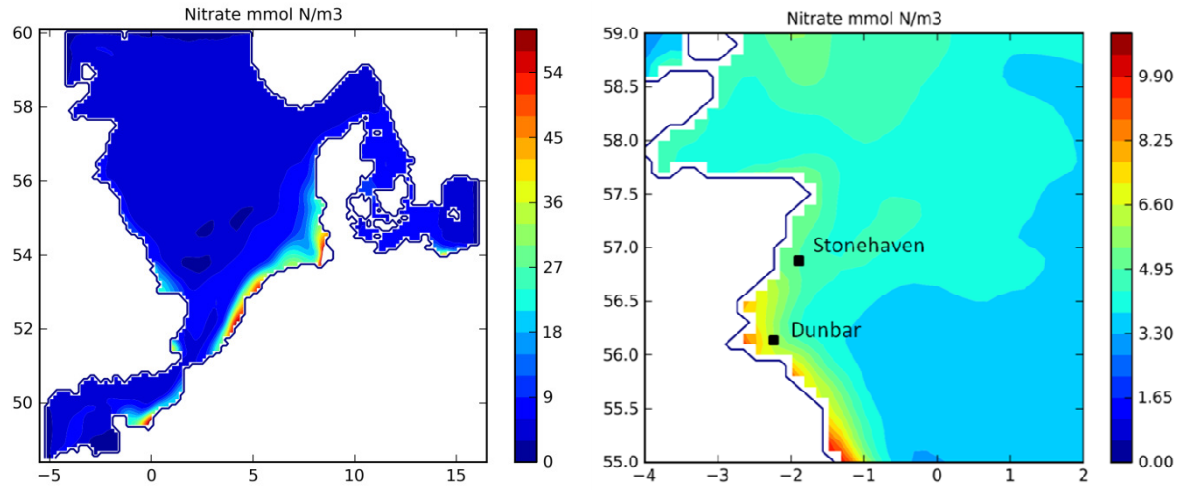

Figure 6: Annual average surface nitrate concentrations, for the whole model domain (left) and for the east coast of Scotland (right), with hypothetical farm locations. Note the difference in colour scales.

3 Results

3.1 Compartment model with macroalgal sub-model

Different scenario calculations were set up for the CKP model as follows: for each generic site an initial run was carried out using the equivalent region with no macroalgal production, a specified boundary nutrient curve and assuming zero net exchange of phytoplankton at the boundary. The result was a time series representing a seasonal cycle of nitrate and phytoplankton reflecting the nutrient and light characteristics and of the site to be used as boundary conditions for subsequent calculations. Using these boundary conditions, a model run with no macroalgal production was carried out to provide a reference to compare against. Finally the runs with macroalgal production were carried out and results compared against the reference run.

The phytoplankton predictions show reasonable correspondence in the CKP model compared with observations for the Scottish west coast. For example, the characteristics of

the generic west coast site simulated in the model compared favourably with data for Loch Creran (Figure 7). The results indicate that the broad seasonal characteristics can be well reproduced even using the rather simple single component phytoplankton model used in this study. The timing of the main production period in March-April ('spring bloom') is reproduced well, but the phytoplankton chlorophyll concentrations predicted by the model for the generic west coast site are about half the Loch Creran values. This is consistent with the assumed winter nitrogen concentrations of 5 mmol m^{-3} that are about half those reported for Loch Creran (Tett et al. 2011).

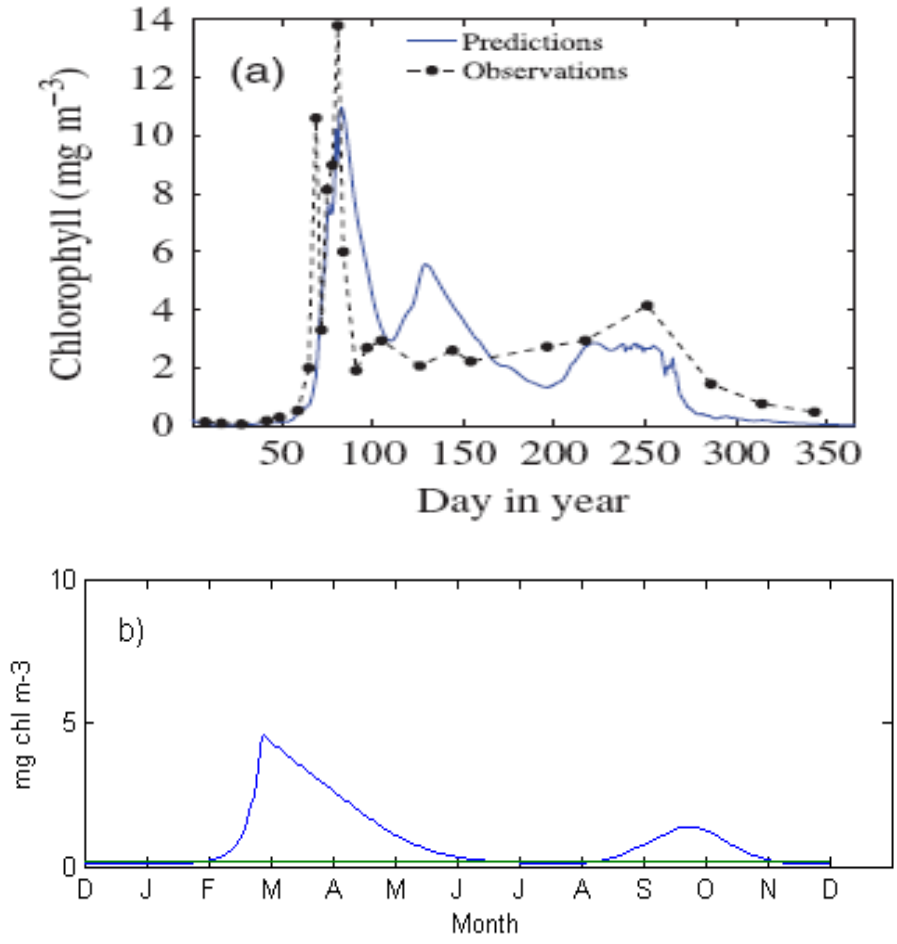

Figure 7: a) Simulated and measured phytoplankton (expressed as chlorophyll) for Loch Creran from Tett et al. (2011). b) CKP model results for generic sites 2, 3, 4 (west coast).

3.1.1 Predicted impacts on phytoplankton and nutrients of macroalgal production

At site 1, the model gave peak dry weight densities in July slightly in excess of the target value of 2000 g dry weight m^{-2} (Figure 8c). As noted before, this required the starting density of macroalgae to be set to a sufficiently high value. Large local impacts on phytoplankton were predicted, with annual average chlorophyll concentrations decreased by 50% within the production area, decreased by 30% within the middle compartment, and decreased by around 10% in the outer compartment representing a minimum distance of 7.5 km from the edge of the production area (Table 3, Figure 8b). Similar reductions in annual average water nitrate concentrations were also predicted (Table 3, Figure 8a).

For the generic west coast sites 2,3 and 4 and beginning the simulation with the same initial macroalgal densities as site 1, predicted peak macroalgal dry weight densities were around 1400 g dry weight m^{-2} (Figure 9). Again large local impacts on phytoplankton were predicted. A comparison of the model prediction for the two generic sites showed clearly the difference in winter nutrient concentrations and consequent effects on phytoplankton chlorophyll concentration and macroalgal dry weight (Figure 10). The more favourable underwater light transmission assumed for the west coast sites 2, 3 and 4 caused an earlier spring bloom in the phytoplankton. It is likely that this also acted to reduce the peak macroalgal biomass as the kelp had a shorter period of time in which it could take up nutrients from the water column before having to rely on internal reserves. Nevertheless, the relative impacts on phytoplankton and nutrient concentrations were very similar to the Clyde site (Table 3) with similar relative reductions at given distances from the production area.

Location	Compartment	Annual average nitrogen concentration (%reduction relative to reference value)	Peak nitrate reduction (%relative to reference value)	Annual average phytoplankton chlorophyll (%reduction relative to reference value)	Peak phytoplankton chlorophyll (%reduction relative to reference value)
Site 1	Outer	6	3	8	15
Site 1	Middle	26	13	25	36
Site 1	Inner	60	32	43	60
Site 2,3,4	Outer	8	4	9	13
Site 2,3,4	Middle	31	19	31	35
Site 2,3,4	Inner	69	48	49	58

Table 3. Relative change to annual peak and average nitrate and chlorophyll concentrations at different distances from the production area (distances should be regarded as minimum for the specified change).

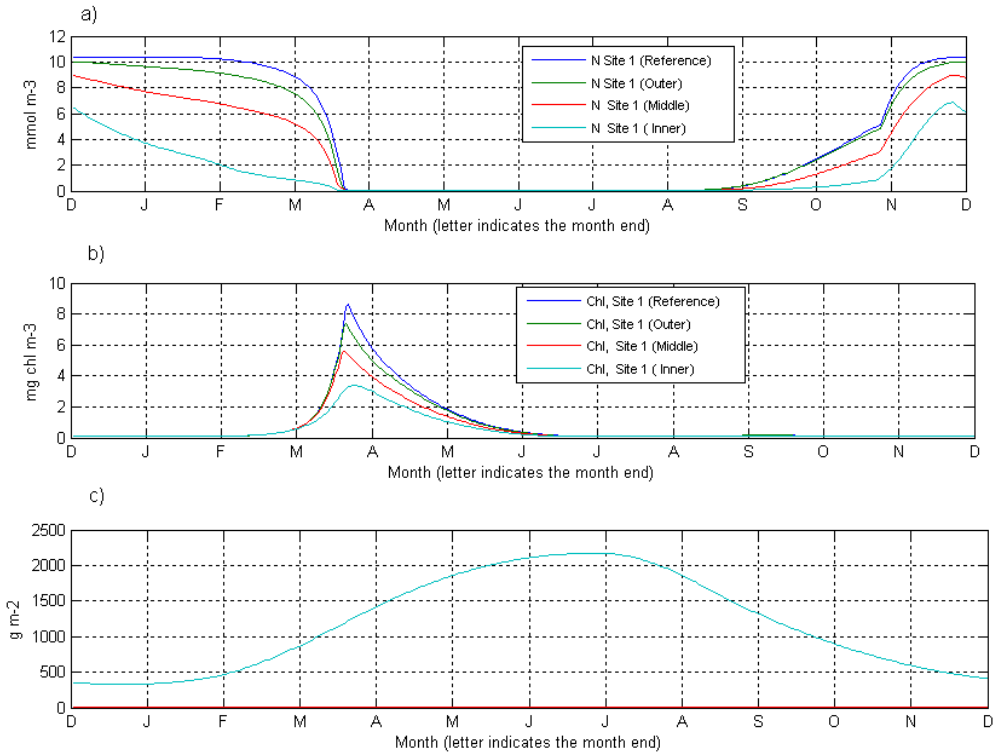

Figure 8: Compartment model results for site 1 for three compartments; 1) Within production site (inner), 2) within 2.5 km (middle), and 3) within 7.5 km (outer) from production area. Plot a) Dissolved Inorganic Nitrogen (nitrate). b) Phytoplankton chlorophyll. c) Average dry weight density within production area.

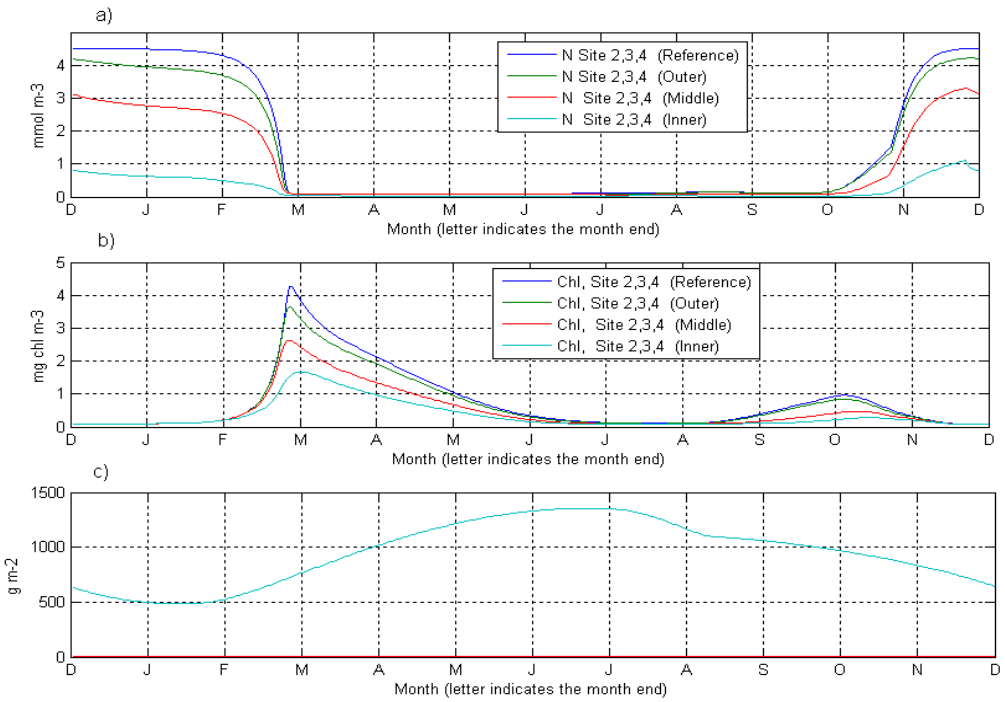

Figure 9: Compartment model results for site 2, 3 and 4 for three compartments; 1) Within production site (inner), 2) within 2.5 km (middle), and 3) within 7.5 km (outer) from production area. Plot a) Dissolved Inorganic Nitrogen (nitrate). b) Phytoplankton chlorophyll. c) Average dry weight density within production area.

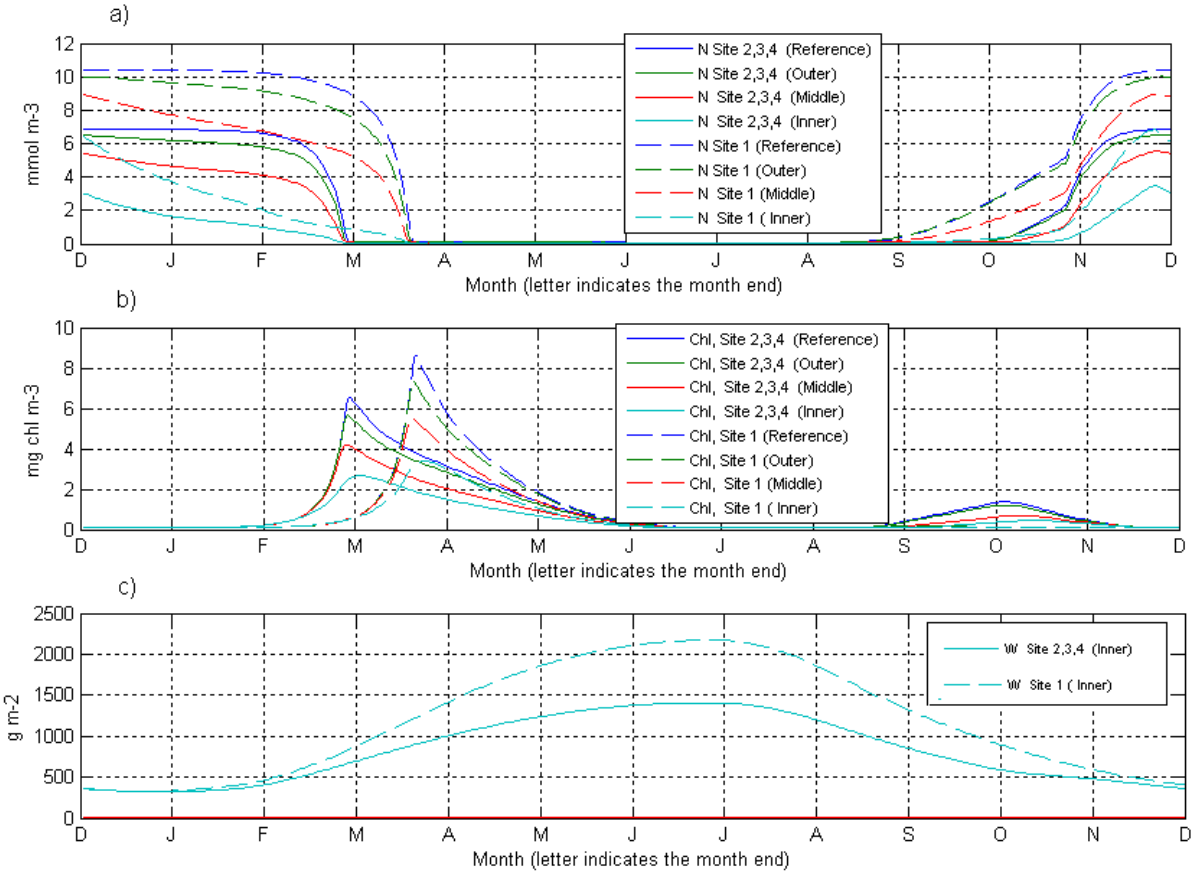

Figure 10: Compartment model results compared between generic site 1 (Clyde) and sites 2, 3 and 4 (West Coast) for three compartments; 1) Within production site (inner), 2) within 2.5 km (middle), and 3) within 7.5 km (outer) from production area. Plot a) Dissolved Inorganic Nitrogen (nitrate). b) Phytoplankton chlorophyll. c) Average dry weight density within production area.

The additional effect on phytoplankton growth by macroalgae shading was found to be minimal (Figure 11) as the phytoplankton were predicted to be strongly nutrient limited such that a reduction in light had little or no effect.

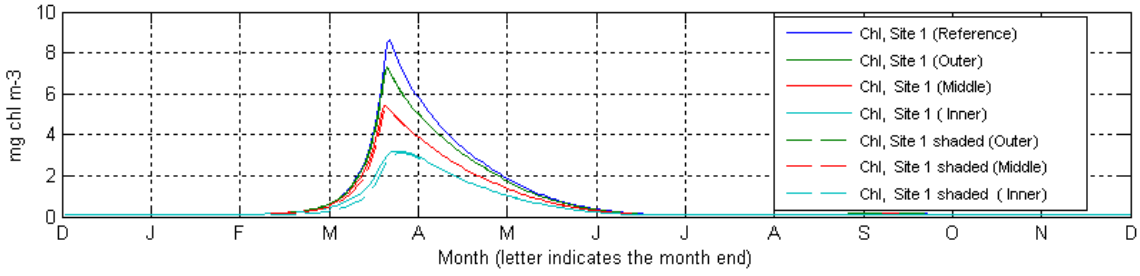

Figure 11: Effect of macroalgal shading on phytoplankton chlorophyll concentrations.

The sensitivity of the CKM model to the inter-compartment exchange rates was investigated. It was found that the exchange rate affected the predicted peak macroalgal biomass so that it was necessary to compensate by adjusting the A_0 value in order that simulations with different exchange tests yielded the same peak macroalgal biomass. Thus, as intended, the results reflect only the sensitivity of the impact to the effects of exchange rates on the transport aspects of the calculation. An increased exchange rate reduced the magnitude of change in mean and maximum chlorophyll and nitrate concentrations. The results suggest that it is the near field in the vicinity of the production area that is most sensitive to assumptions about this parameter (Figure 12, Figure 13). At greater distances the effect of different values for the exchange rate is smaller.

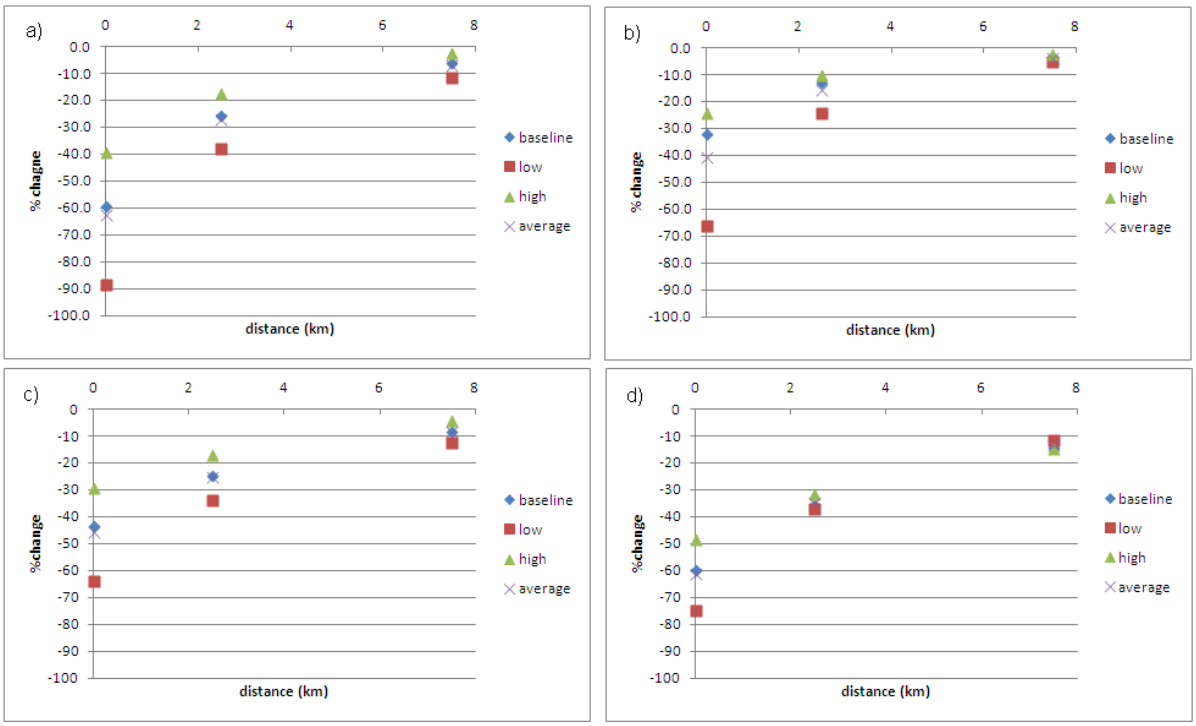

Figure 12: Site 1, relative change with distance from edge of production area for mean and maximum nitrate and phytoplankton concentrations and sensitivity to an assumed high (x1.5), baseline and low (x0.5) values of the inter-compartment exchange rates. a) Annual mean nitrate. b) Annual peak nitrate. c) Annual mean phytoplankton. d) Annual peak phytoplankton.

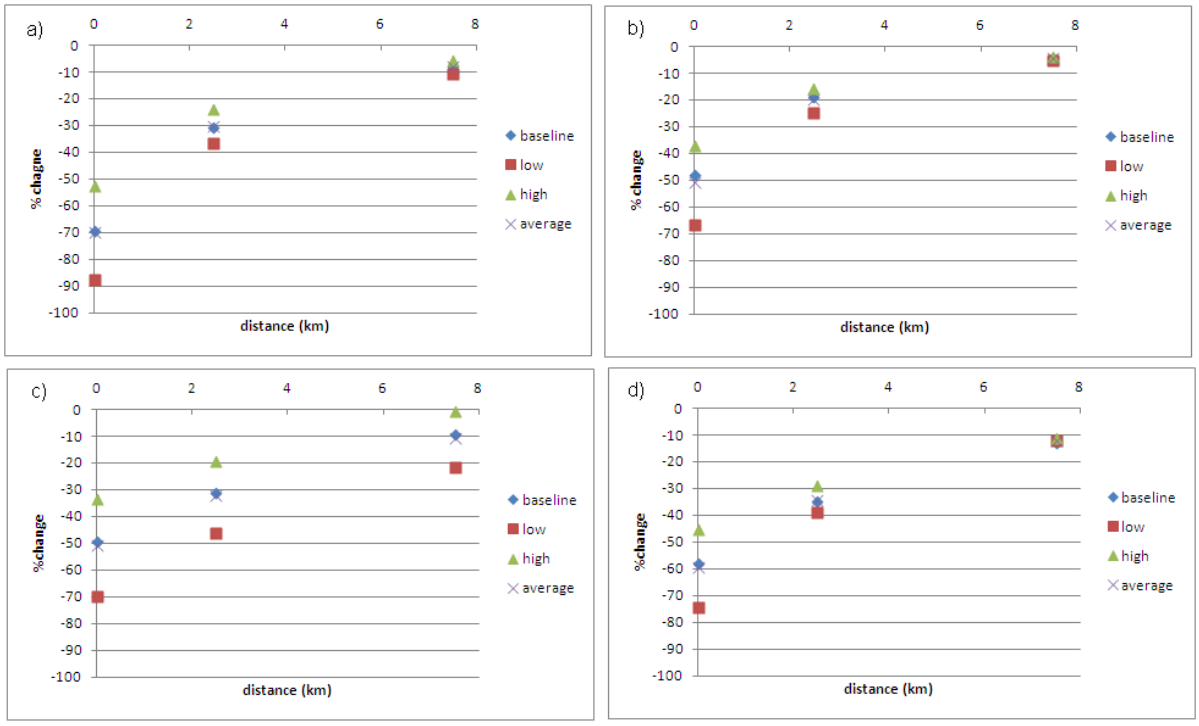

Figure 13: Site 2, 3, 4 relative changes with distance from edge of production area for mean and maximum nitrate and phytoplankton concentrations and sensitivity to an assumed high (x1.5), baseline and low (x0.5) values of the inter-compartment exchange rates. a) Annual mean nitrate. b) Annual peak nitrate. c) Annual mean phytoplankton. d) Annual peak phytoplankton.

3.1.2 Budgets

Budgets of the annual uptake of nitrogen partitioned between phytoplankton and macroalgae (Table 4) show a much elevated demand due to the presence of macroalgae. Interpretation is made difficult because nutrient recycling is occurring so not all the additional nutrient demand from the macroalgae is new nutrients. The lower biomass predicted at the generic west coast site leads to the lower nutrient uptake by macroalgae at this site, although it is notable that the nutrient uptake by phytoplankton at the two sites is of a similar order even though the chlorophyll concentrations are about half the value at the generic west coast site. These calculations indicate that a 20 km^2 kelp farm in the Clyde Sea would extract approximately 480 tonnes of nitrogen from the marine environment per year if operated at the target yield of 20 tonnes dry kelp per hectare.

		Phytoplankton annual nitrogen uptake (mol N m^{-2}) averaged over entire region	Macroalgae annual nitrogen uptake (mol N m^{-2}) in inner region
Site 1	No macroalgae	0.30	0.0
	With macroalgae	0.24	1.6
Site 2,3,4	No macroalgae	0.30	0.0
	With macroalgae	0.24	1.0

Table 4: Nitrogen budgets from the combined kelp phytoplankton model. The values are per unit area of the region where the species is present. For phytoplankton this is the entire region, for macroalgae it is the inner region only.

3.1.3 Exudates

The CKP model indicated that up to 4 g C m^{-2} d^{-1} was fixed by *S. latissima* blades, leading to a harvestable biomass of 2000 gC m^{-2} by mid-summer. Macroalgal carbon loss rates can vary between 12.5 and 100% of the net production rate. This would give a total carbon loss to the environment of between 0.5 and 4 g C m^{-2} d^{-1}, which, depending on its composition, may sink quickly and be confined to the immediate area of the farming operation (inner compartment) or may be dispersed throughout the surrounding area by advection. It is assumed in both cases that all macroalgal carbon was (1) transferred to a benthic mixed layer of depth 15 m (2) was bioavailable, (3) was respired immediately by heterotrophs, and (4) consumed oxygen with a respiratory quotient of 1. Furthermore, it was assumed that oxygen concentration in the BML was fully saturated at the onset of the model run (265 mmol O_2 m^{-3}) giving a total available oxygen supply of 4.0 mol m^{-2} in the BML. A simulation was run for 90 days to simulate the extent of the stratified period during summer when oxygen depletion is most likely to occur.

In the absence of horizontal flushing through the BML, then the input of a biolabile carbon source to the BML immediately below kelp production area would result in complete consumption of the oxygen supply within 13 days for the a carbon exudate production of 4 g C m^{-2} d^{-1}. Lower inputs of carbon gave correspondingly lower consumption of oxygen: at the

lowest carbon exudation rate of 0.25 g C m^{-2} d^{-1} oxygen concentration remained above 50% saturation for 49 days.

Horizontal flushing rates of over 0.2 d^{-1} were sufficient to maintain oxygen concentrations in the BML under the production unit at over 50% even for the highest input of carbon (Figure 14). Lower flushing rates were insufficient to maintain adequate oxygen concentrations when the carbon input was 2 g C m^{-2} d^{-1} or above.

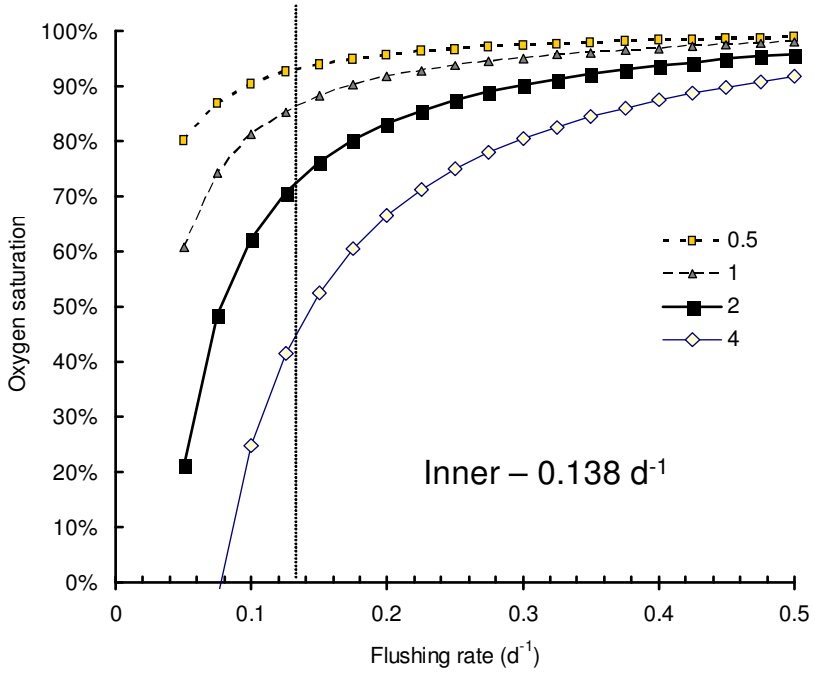

Figure 14: Oxygen reduction assuming lost material is concentrated below farm area (20km^2). Steady-state benthic mixed layer oxygen concentration for the 'inner' compartment is expressed as percentage saturation relative to air-saturated seawater at 10°C under different combinations of carbon input and flushing rate. The dashed vertical line shows the flushing rate used in the CKP model.

In a second scenario, inputs of biolabile carbon were allocated across the BML of the farm itself (20 km^2) and its immediate surrounding area of 60 km^2 (see Figure 4). The greater volume of water in the receiving body results in a proportionally lower effect on steady-state oxygen concentrations (Figure 15). A flushing rate of 0.05 d^{-1} was sufficient to maintain BML oxygen at over 50% even with the maximum carbon input of of 4 g C m^{-2} d^{-1}.

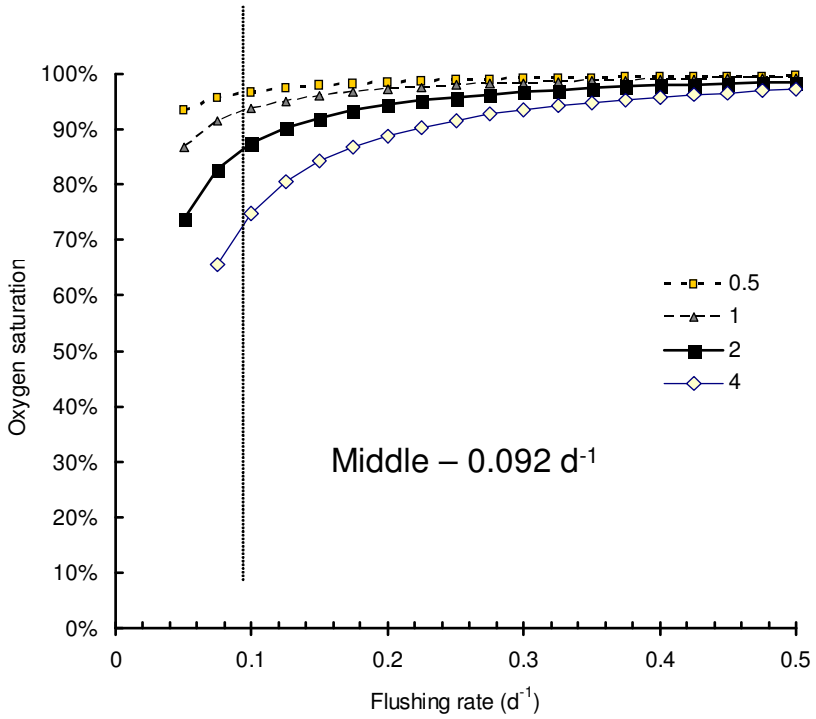

Figure 15: Oxygen reduction assuming lost material is concentrated below farm area+middle region (20+60 km^2). Steady-state benthic mixed layer oxygen concentration for the 'inner+middle' compartment is expressed as percentage saturation relative to air-saturated seawater at 10°C under different combinations of carbon input and flushing rate. The dashed vertical line shows the flushing rate used in the CKP model.

3.1.4 Volatile gases

Brown seaweeds, and kelps in particular, use a variety of halogenated organic compounds in their metabolic pathways. These compounds confer a moderate protection to oxidative stress and may function as anti-grazing agents. The *Laminaria* genus can concentrate iodine at internal concentrations of up to 30 000 times higher than the surrounding seawater (Nitschke et al. 2011). Volatile iodated compounds are held in cells near the surface of the stipe and lower parts of the blade (Kuepper et al. 2008), and release of large quantitites of iodine can be triggered by mildly stressful events such as the tidal exposure to air during daytime. The iodated compounds such as iodide (I^-), iodine oxide (IO) and methyliodide (CH_2I_2) produced by intertidal kelp beds can clearly be measured in the lower atmosphere in the marine-terrestrial transition zone, particularly so at sites of high

macroalgae density (Roscoff, France and Mace Head, Ireland; Leigh et al. 2010). The quantities of carbon released in this process are minor compared to that stored in the blade or lost as exudates. For example, release rates of methyliodide for a dense surface canopy of the giant kelp *Macrocystis pyrifera* were calculated as less than 1 mg Ch3I m^{-2} d^{-1} (Manley & Destoor 1987).

Organohalogens are however important in atmospheric chemistry. Methyliodide, methylchloride and methylbromide all have significant natural sources in the ocean from macroalgae and phytoplankton (Carpenter & Liss 2000), and can breakdown to release highly reactive free halides in the atmosphere. Chlorine is an efficient catalyst in the conversion of ozone to molecular oxygen. Iodine oxide is the compound released in the greatest quantities from kelp exposed to stress conditions (exposure to high irradiance, desiccation). Upon release from the thallus in the presence of sunlight, IO forms ultrafine aerosol particles in the air above and downstream of the exposed kelp bed (Kuepper et al. 2008). These 'coastal particle bursts' can aggregate to form cloud condensation nuclei thus affecting the formation of coastal clouds (Whitehead et al. 2009).

3.2 GETM-ERSEM-BFM modelling

3.2.1 Validation

Model results of nutrient concentrations at the Stonehaven site were compared with observations for the years 2004-2008 (Figure 16). These results show reasonable to good agreement for nitrate and phosphate. Both the model results and the observations showed little sign of stratification, in contrast to the sites on the Scottish West coast simulated with the CKP model. Ammonium values were of the right magnitude, but the temporal distribution did not correspond with observed data with the exception of the year 2005. As ammonium concentrations are difficult to model, this is considered to be a reasonable result. Silicate values tended to be over-predicted by the model by a factor of 2. As silicate was only marginally limiting in the observations, and only of importance for diatoms, this over-prediction is not expected to have a large effect on the model results for this site.

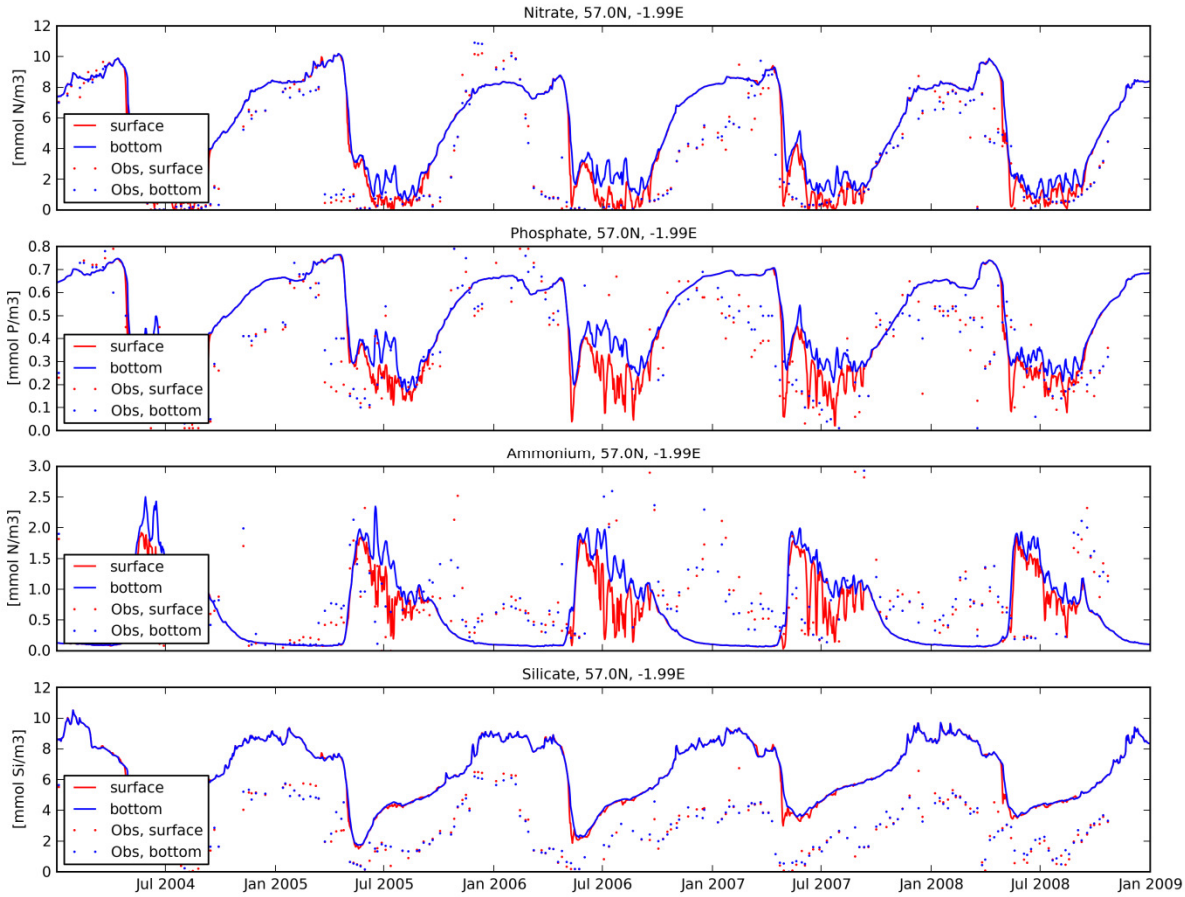

Figure 16: Comparison of model results of nutrient concentrations from the reference run with observations at the Stonehaven site (George Slesser, pers. comm.)

3.2.2 Scenarios

3.2.2.1 Reference scenario

The reference conditions were derived as depth-integrated, annual averaged values, subsequently averaged over the last 4 years of the simulation (2005-2008) for a number of pelagic chemical, phytoplankton related, zooplankton related and benthic variables (Appendix C: ERSEM-BFM model results). Integrating over depth allows for interpretation in terms of total amount available at any location, but because of the large differences in depth across the North Sea, the resulting plots look different from e.g. equivalent plots of surface concentration. As a result, riverine plumes of phosphate and nitrate do not show as prominently as they would do if concentrations were plotted. These reference conditions show very different spatial patterns for the different biogeochemical variables in the model. Discussion and understanding of these patterns are beyond the scope of this report. The

main cause and effect relations are that (i) phytoplankton grows where nutrients and light are available, with different characteristics for the separate functional groups, that (ii) zooplankton thrives where there is food (phytoplankton and/or other zooplankton) available for them, again with different characteristics for the functional groups, and similarly for the benthic groups. For all these functional groups, temperature and other environmental factors influence the growth and mortality. These results are intended as background information to help explain the differences resulting from the different macroalgae farm scenarios (below; see Section 2.3.3 and Table 2 for a description of the scenarios simulated with the 3D model).

3.2.2.2 Scenario 6: time series of nutrient sinks for Stonehaven

To illustrate the seasonal variations and magnitude of the nutrients extracted by the macroalgae (Appendix B: Implementation of nutrient sink in ERSEM-BFM), time series are given for Scenario 6 as daily averages (Figure 17). For this scenario, the maximum uptake for unlimited, very high nutrient concentrations is $U = V_{max}*A$ = (12, 120, 120) $mmol\ m^{-2}\ day^{-1}$ for phosphate, nitrate and ammonium, respectively. The modelled uptake was less than expected because of lower actual nutrient concentrations. The results show highest nutrient uptake during approximately 8 months in autumn, winter and spring, and low uptake during approximately 4 months in summer. Summer uptake was a mixture of nitrate and ammonium. Annual budgets for this scenario (6), and also for Scenarios 1, 2 and 4 (see Section 2.3.3, Table 2 for scenario definitions) in terms of nutrients extracted per unit area are given in Table 5 for 2005-2008.

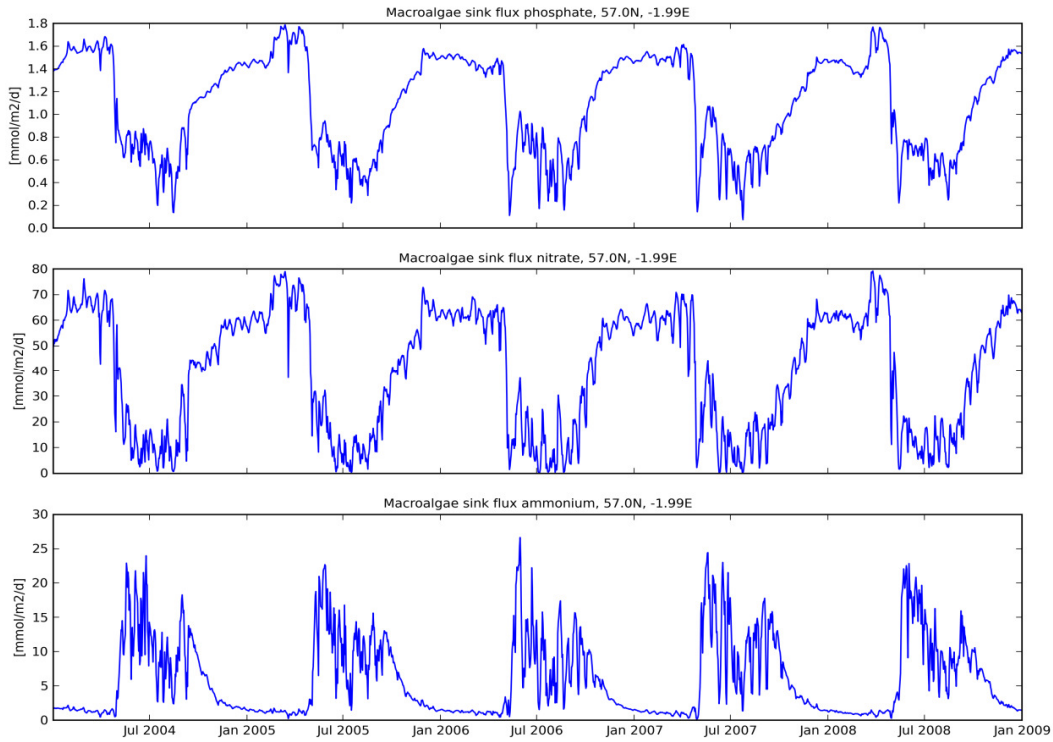

Figure 17: Nutrients extracted as a function of time at the Stonehaven site for a farm with intensity A=500 dm^2/m^2.

Annual budget [mol/m^2]	Phosphate				Nitrate				Ammonium			
Scenario	2	1	6	4	2	1	6	4	2	1	6	4
A [dm^2/m^2]	50	100	500	1000	50	100	500	1000	50	100	500	1000
2005	0.046	0.091	0.410	0.731	2.073	3.998	15.257	22.502	0.411	0.748	2.190	2.872
2006	0.045	0.088	0.397	0.705	1.986	3.818	14.524	21.171	0.384	0.689	1.981	2.613
2007	0.044	0.086	0.385	0.684	1.955	3.749	13.826	19.929	0.408	0.743	2.267	3.065
2008	0.046	0.090	0.408	0.730	2.054	3.963	15.268	22.582	0.402	0.735	2.196	2.928

Table 5. Annual budgets for GETM-ERSEM, in terms of nutrients extracted per unit surface area, for a farm at the Stonehaven site with intensities A=50, 100, 500, 1000 dm^2/m^2.

3.2.2.3 Scenario 4: highest density farming

For scenario 4, the relative difference with the reference scenario was up to 20% for some variables (Appendix C: ERSEM-BFM model results). Relative differences were even higher for a selection of variables in the immediate vicinity of the farm. However, other

variables showed only minor changes. Phosphate and nitrate, and to some extent ammonium showed the strongest response in the vicinity of the farm. The other variables showed the maximum response away from the farm. Benthic variables seemed relatively sensitive to pressures generated by the uptake of nutrients from the farm, with differences of up to about 40%. Most variables showed a response along the UK east coast up to northeast Norfolk, in line with the prevailing residual circulation (e.g. http://chartingprogress.defra.gov.uk/sea-temperature-salinity-and-circulation and references therein). Some variables had the strongest response in an area between the Humber and north Norfolk coast (i.e. CO_2 and pH, dissolved inorganic carbon, *Phaeocystis*, most benthic variables).

Most variables showed a reduction in concentration or biomass, but some showed an increase in part or all of the area affected. In particular, *Phaeocystis*, an inedible nuisance algae, blooms of which can be associated with eutrophication, showed a relatively strong decrease in abundance along most of the east coast, where it was replaced by pico-phytoplankton, which thrives in more oligotrophic conditions. In general, the model predicted shifts in species composition, but comparatively smaller changes in overall primary and secondary production.

These relative differences of modelled variables in the results of the scenario simulations should be treated with some caution, as small absolute changes in areas with very low reference levels can lead to a large relative difference, which may not be very meaningful.

3.2.2.4 Response to farming intensity

The response of nutrients to differences in farming intensity at the Stonehaven site (scenarios 1, 2, 4 and 6, Figure 18) showed an effect on the magnitude of the response, but this did not significantly affect the spatial distribution. For the lower farming-intensity scenarios, the results showed an additional, patchy response in the central North Sea. This is related to a high sensitivity of the stratification in the area of the Norwegian Trench to (minor) changes in forcing, and may be a model artefact related to the limited vertical resolution for these deeper areas that needs to be investigated further. Results from this

area were not thought to affect the general patterns in the area of direct interest (east coast of the UK) because of the general directions of the residual circulation.

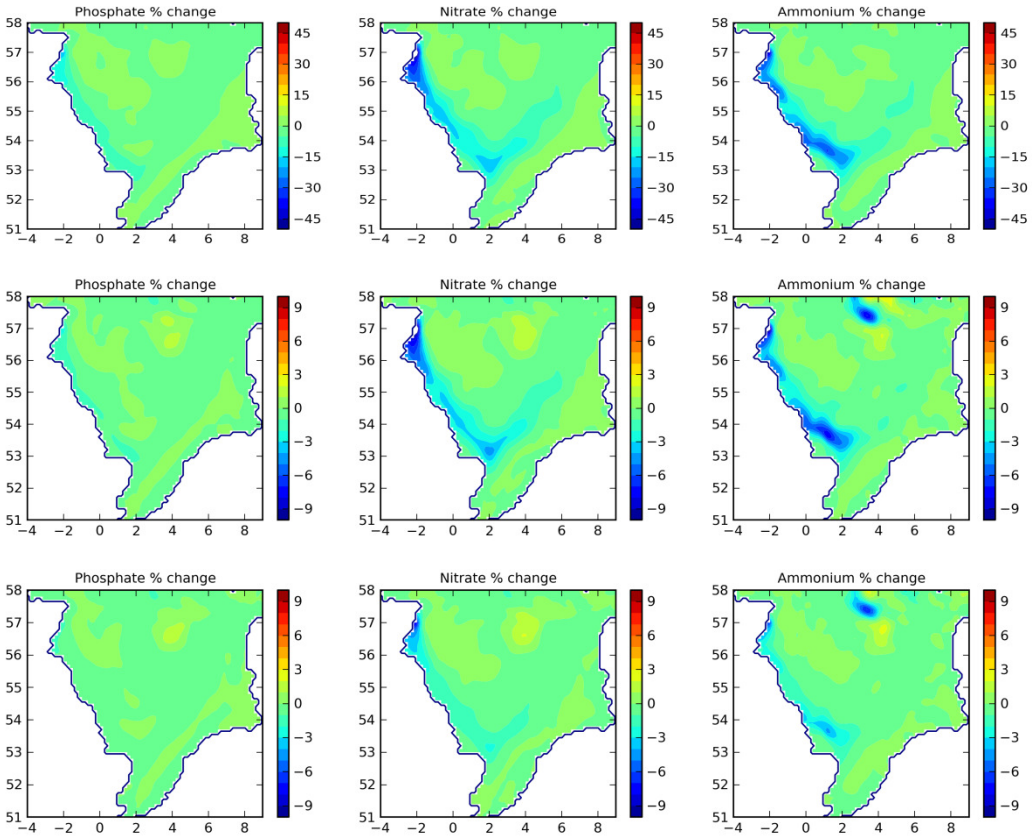

Figure 18: Relative change in depth-integrated, annual averaged nutrient concentrations for different intensities of farming: A=1000 dm^2/m^2 (top row), A=500 dm^2/m^2 (second row), A=100 dm^2/m^2 (third row), A=50 dm^2/m^2 (bottom row).

Look-up graphs were constructed based on the results for the Stonehaven site that give the surface area affected down to a percentage as a function of the macroalgae farm intensity *A* for nutrients, primary and secondary production, and filter feeder biomass (Figure 19). These graphs can be used to obtain a first impression of the potential impact of hypothetical farms situated in a similar setting. The results suggest that (i) small impacts of <10% change occur over larger areas, whereas more severe impacts (a change > 20%) tended to occur at much smaller scales, and (ii) that pelagic variables were progressively less affected with increased trophic level, while benthic variables (through the suspension feeders) were relatively sensitive. However, large percentage changes in suspension feeder

biomass were simulated over substantial areas with very low suspension feeder biomass (Appendix C: ERSEM-BFM model results), so the significance of the latter result is likely to depend on the context and should be treated with caution.

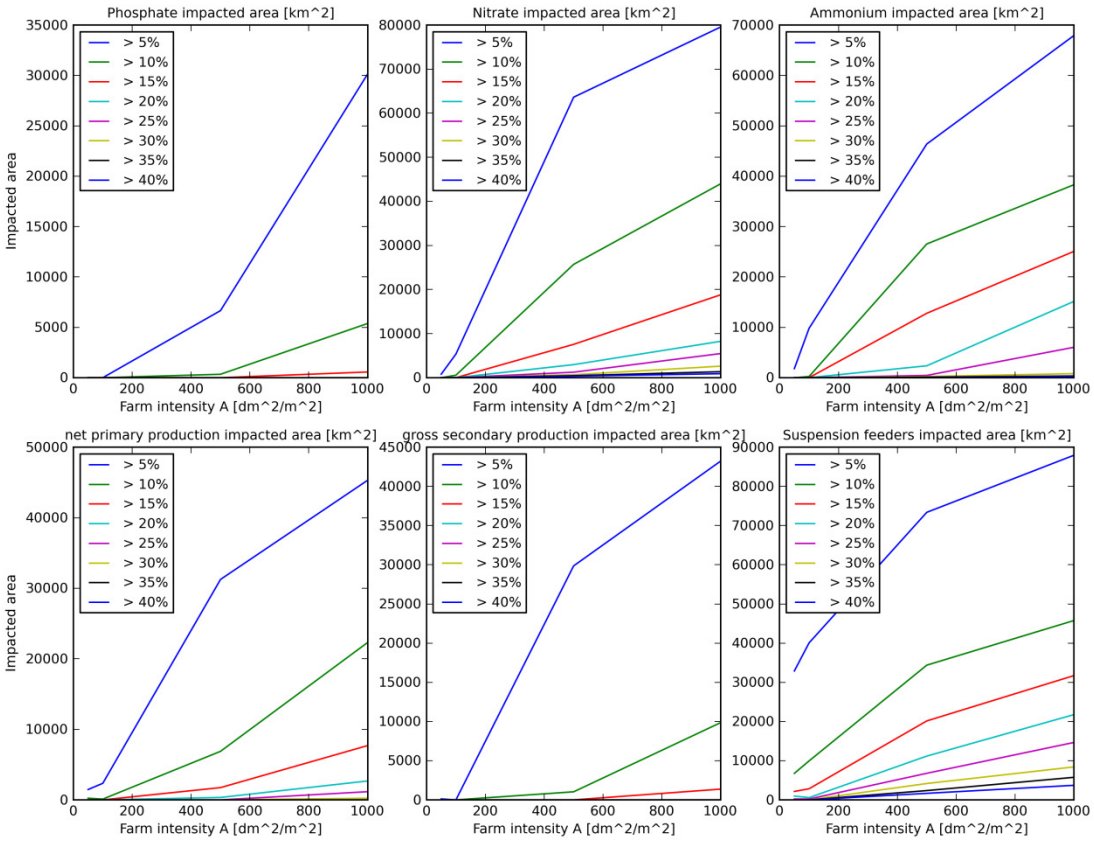

Figure 19: Area affected as a function of farming intensity (A) for phosphate, nitrate, ammonium, net primary production, gross secondary production and filter feeder biomass. The lines indicate percentage of change (positive and negative taken together) of the variable. So for example for ammonium, for a farming intensity of 400 dm^2/m^2, 40000 km^2 had a change of more 5% or more in annual average, depth-integrated concentration, 20000 km^2 a change of 10% or more, and so on.

3.2.2.5 Response to farm location

The farm location (scenarios 4 and 5) only affected the changes in nutrient concentrations in the vicinity of the farms (Figure 20). The far-field down-stream effects were similar. This result also held for the other variables in the model (not shown).

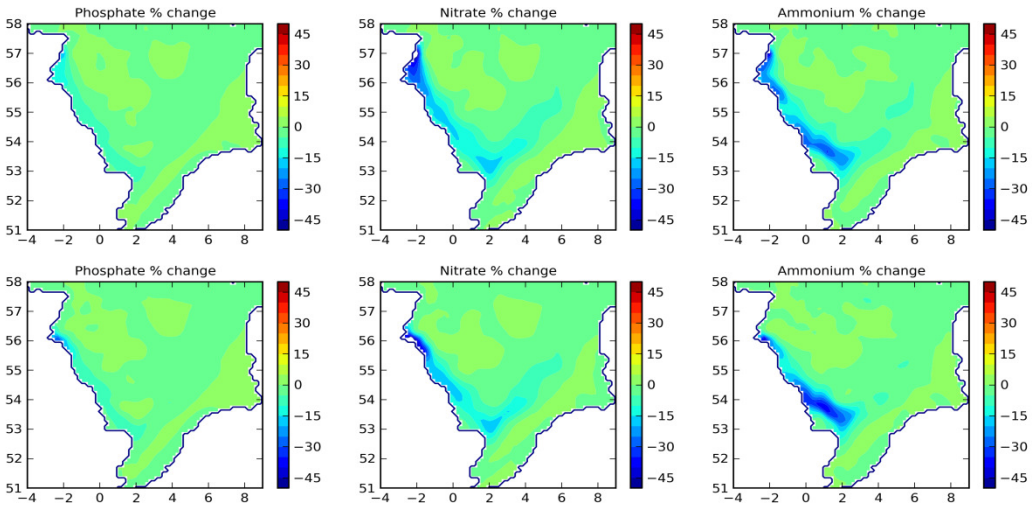

Figure 20. Relative change in depth-integrated, annual averaged nutrient concentrations for A=1000 dm^2/m^2 for the Stonehaven site (top row), and for the Dunbar site (bottom row).

4 Discussion

4.1 Compartment model results

The CKP model was set up and calibrated for the kelp *Saccharina latissima* and was able to reproduce the main features of measured data for this species as presented by Sjøtun (1993). Other species of interest include *Laminaria hyperborea* and *Laminaria digitata*. It is argued that the characteristics leading to the main wider scale impact, uptake of nutrients during the late winter period and production of organic carbon detritus, are common to all three species and that the focussing on *Saccharina latissima* is adequate to assess this impact. The three species have similar characteristics during the first year of growth, and species-specific differences become apparent with increasing age, particularly in the canopy-forming mature *L. hyperborea*.

The results from the CKP compartment model indicated very significant impacts on phytoplankton in the vicinity of the macroalgal farm area, where mean chlorophyll would decrease by 40-50%. Relative decreases in phytoplankton concentration were predicted to be greater than 10% at distances in excess of 7.5km from the edge of the farmed area. This was found to be the case at both the Clyde site (site 1) and the generic west coast site (sites 2, 3, 4). The main reason for the decrease in phytoplankton biomass appeared to be competition between seaweeds and phytoplankton for nutrients. Winter nutrient uptake by the macroalgae caused a decrease in nutrients available for the spring phytoplankton bloom. The additional effect on phytoplankton of shading beneath the macroalgal layers in the farm area was found to be of minor consequence as the phytoplankton were already strongly limited by nutrients in this situation. It has been shown across a range of coastal ecosystems that the standing stock of consumers is directly dependent upon annual primary production (Herman et al. 1999). It is to be expected that any decrease in primary production in and near the farm site would be expected to result in relative decreases in the zooplankton and filter-feeding benthic animals of that area. The magnitude of this decrease would be site-specific, depending on the types of herbivores present and their seasonality. The overall productivity of an area (e.g. seaweeds plus phytoplankton) would be increased by farming, but the organic material produced would be in a different form (e.g. exudates

and litter rather than diatom cells). Organisms such as detritivores and omnivores would potentially benefit, whereas filter feeders and zooplankton may show reduced abundance.

It should be emphasised that the simple spatial structure of the model setup did not allow the directionality of impacts to be addressed. The distances associated with the predicted impacts were based on a uniform dilution in all directions. In reality the area of impact would be expected to be elongated in the direction of the residual transport[4] with the impact distances higher in that direction and smaller in the opposite or perpendicular directions. Estimation of this behaviour would require a more sophisticated representation of transport processes with site specific bathymetry and hydrodynamics. In the absence of such a model it is difficult to estimate the influence of the residual transport, although the distance that a given reduction in phytoplankton concentrations occurred could be several times larger in the residual flow direction than would be suggested directly by the compartment model results. Indeed, the calculations with GETM-ERSEM reported here suggest that the distances of impact may be considerably more than that suggested by the simple compartment modelling approach.

As well as the impact on nutrients and phytoplankton the potential effect on oxygen concentrations of the breakdown of organic material such as exudates released by macroalgae were investigated. The rates of both particulate and dissolved carbon loss are high due to the particular characteristics of kelps, where the meristematic region of the blade grows constantly and the distal end of the blade sheds material. The CKP model showed that loss rates are particularly high over the summer period when external nutrient concentrations were at the lowest point. A set of simplifying assumption were made to examine the biological oxygen demand of kelp material lost from an operational farm located in a thermally-stratified water column. If the lost kelp production were to be deposited to the seabed directly under the farm then moderate to severe oxygen depletion would be predicted unless horizontal flushing rates were sufficient for replenishment. Dispersion of kelp material across a wider area would proportionally reduce the oxygen demand. It would seem unlikely that effects would be noticeable at distances beyond 7.5

[4] In some regions a well defined residual may not exist but may be variable depending on meterological or freshwater runoff.

km from the farm perimeter. These results may be useful for siting of a farm: areas of high advective current flow, and no or weak stratification would be favoured over low-flow, stratified areas. The timing of kelp harvest in early summer would also be important to maximise yields and minimise losses of carbon to the environment.

4.2 GETM-ERSEM-BFM model results

The model results suggested a reduction of 10% or more in depth-integrated nutrient and chlorophyll concentrations over an area of several tens of thousands of square km for the highest intensity farming scenario that was simulated, reducing to nearly zero square km for the lowest intensity simulated. The highest intensity scenario assumed a macroalgae yield per unit area corresponding with a realistic operational farm, with high density packing of algae across the site. The parameter A used to describe the farming intensity is equivalent to the 'leaf area index' (LAI) which has been used to describe natural kelp communities. The highest values of LAI of 4- 5 units are recorded for *L. digitata* and *S. latissima* just below the low tide line (Luning 1969). This is equivalent to an A value of 400-500 dm^2 m^{-2}, similar to our scenario 6. However, because the intensity of the operation was applied over a larger area (114 km^2) than currently expected for a single farm (10-20 km^2) this situation can be assumed to be an extreme example. If multiple farms were to be built, and if these farms were situated down-stream of each other so that they effectively extract nutrients from the same water masses, it is possible that their cumulative impact could reach the simulated worst case scenario.

The model ignored the influence of light shading by the macroalgae on phytoplankton. As phytoplankton can survive low light conditions for a while, this simplification is expected to have only shifted the model results for primary production by one horizontal grid cell in the vicinity of the simulated farm, resulting in only minor changes. This interpretation appears to be confirmed by the CKP model results discussed above.

Since the approach adopted only considered the impacts of nutrient extraction no attempt was made to calculate the additional generation of detrital material using the 3-D model. As described above, carbon losses may be substantial leading to changes in detrital,

bacterial and oxygen concentrations in an area downstream of the farm, including impacts on the benthic system. Nitrogen losses appear to be less important, as kelps actively translocate valuable N away from the distal end of the blade to support the growing areas. The detailed effects of losses of organic material, and its subsequent transport pathways and re-mineralisation or burial in sediments could be investigated as part of further work by incorporating a complete macroalgal model within the ERSEM.

The simulated impacts in terms of nutrient extraction are likely to be an overestimate of the real impact of a macroalgae farm (except for impacts that might be caused by macroalgae-derived detritus), because the grid cell with a nutrient sink simulating the presence of a macroalgae farm in the GETM-ERSEM-BFM model removed all the nutrients that were available to the macroalgae from the ecosystem. In reality, a proportion of these nutrients may be returned to the ecosystem as detritus through mortality, degradation, etc. before the macroalgae can be harvested. Simulating this generation of detritus would require a more complete macroalgae model to be implemented in ERSEM-BFM, because it would need to resolve carbon components the magnitude of which cannot easily be estimated from a simple nutrient sink. Further developments are expected in this area by our partners working on developing a macroalgae model for ERSEM-BFM at NIOZ, Texel, The Netherlands.

Furthermore, the simulated impacts may be an overestimate of realistic cases because a constant, year-round coverage of macroalgae was assumed at densities that (at least for the most intensive farm scenario) might be interpreted as the density at the time of harvest. This assumption might be improved upon by adopting prescribed functional descriptions of macroalgae growth during the season, or by implementing a dynamic macroalgae model.

4.3 Combined model results

Two very different models were used to investigate whether macroalgae farming may have significant impacts on the marine environment. The models were used to investigate different aspects of the problem, using their respective strengths. However, for both models, different assumptions had to be made within the scope of this study which

limited their capability to provide a full, accurate forecast. The results can, however, be combined to infer a more complete estimate of the significance of the impacts. This is summarised below.

4.3.1 Strengths and weaknesses of the different modelling approaches employed

The CKP compartment model contains a relatively sophisticated description of macroalgae growth, specifically designed for the purpose of this study. However it has only a simple, single-group phytoplankton model, and a crude nutrient regeneration mechanism. The benthic system is represented by a nutrient sink, and the hydrodynamics are represented by a horizontal diffusion process. Hence it is good at predicting macroalgae growth and nutrient cycling processes associated with it, but weaker at estimating details of spatial impact or secondary impacts on the ecosystem. Moreover, it has short run times, enabling large numbers of runs required for sensitivity testing.

The GETM-ERSEM-BFM model contains state-of-the-art 3D hydrodynamics and multiple phytoplankton, zooplankton, benthic and bacterial functional groups. For the purpose of this study, it was fitted with a simple nutrient sink to represent the presence of macroalgae. Hence it is good at predicting spatial impacts and secondary impacts on the ecosystem, but weaker at estimating the magnitude of the disturbance which depends on macroalgae growth and nutrient and carbon cycling processes associated with it. A single run with the 3D model takes several days on a parallel computing cluster, and requires substantial amounts of storage, making it less suitable for sensitivity studies.

4.3.2 Magnitude of the nutrient extraction

On an annual basis, the CKP model extracted a similar amount of nutrients as the Galician *Undaria* experimental farm described earlier (1.6 vs 0.8 mol N m^{-2}). The nutrient extraction by the GETM-ERSEM model for a similar farming intensity (A=500 dm^2/m^2) for similar background winter-nutrient concentrations was 10 times higher. Even the lowest intensity (A=50 dm^2/m^2) simulation with the 3D model resulted in higher annual nitrogen

extraction than the compartment model and the experimental farm (2 mol N m^{-2}). The main reasons were:

1. The macroalgae growth model in the CKP model contains a term which limits nutrient uptake depending on the amount of nutrients already stored within the plants, reducing uptake in mid to late winter compared to the formulation of the nutrient sink in the 3D model.
2. The macroalgae growth model in the CKP model allowed for varying plant size/density throughout the season, reducing nutrient uptake in winter when densities were lower as compared with the 3D model.
3. In the CKP model, a proportion of the nutrients taken up by the macroalgae were returned to the ecosystem as detritus, whereas all nutrients extracted through the nutrient sink in the 3D model were removed from the system.
4. The CKP model had a fixed mixed layer depth, whereas observations show that this depth can be highly variable over the year. Hence, the availability of nutrients to the macroalgae and phytoplankton may be more complex than that described here.

GETM-ERSEM nutrient extraction rates are sensitive to the specified maximum uptake values and a range of these are presented in the literature. There is therefore a large uncertainty associated with this parameter. The macroalgal component of the CKP model is relatively insensitive to this parameter because of the feedback with internal nutrient concentrations included in that model. As the differences between the models effectively result in different scenarios, the exact difference in uptake cannot be given, but the results of the compartment model are probably more reliable for this aspect, implying that the GETM-ERSEM model most likely over-estimated the impact in terms of annual nutrient uptake substantially. Hence, the results for a modelled farm with intensity A=50 dm^2/m^2 over 10.1x11.1 km^2 probably gives a more realistic representation of the impact of farming activity equivalent to that proposed by The Crown Estate. For a very large scale macroalgal farm, as mentioned by the DECC Carbon Calculator in their ‘marine algae x4 scenario’, then the higher GETM-ERSEM calculations would become relevant.

4.3.3 Spatial extent of the impact on the ecosystem

The spatial extent of the impact on the ecosystem simulated by the GETM-ERSEM-BFM model was larger than that simulated by the compartment model, because:

1. The residual flow structure simulated by the 3D model was more or less uni-directional, allowing primarily for nutrient supply from the up-stream direction, while carrying waters with reduced nutrient concentrations down-stream with very limited lateral replenishment. In contrast, the diffusion mechanism in the compartment model allowed for nutrient transport in all directions, allowing a higher level of replenishment of waters where nutrient concentrations were reduced because of the presence of macroalgae.
2. The compartment model was only run for a year, as it had a relatively short response time because of the lack of a benthic system and spatial processes. The 3D model, in contrast, was run for 15 years to allow for the flushing time of the North Sea (several years, e.g. Otto et al., 1990), and for the response time of the benthic system (up to a decade), resulting in a cumulative, equilibrated impact.

Hence, the (smaller, several tens of km) spatial footprint suggested by the CKP model is more representative of short-term (intra-annual) effects for locations with weak uni-directional trends in hydrodynamics, whereas the (larger, hundreds of km) spatial footprint suggested by the 3D model is more representative of the long-term (decadal) effects of sustained operation of a macroalgae farm in locations with strong uni-directional trends in the hydrodynamics. As the shape of the spatial distribution (as opposed to the magnitude) of the impact in the 3D model did not depend very much on the imposed farming intensity, these conclusions are expected to hold also if an improved nutrient uptake mechanism were implemented. Spatial maps of the relative difference of the model results for the Stonehaven site with intensity A=100 dm^2/m^2 (annual extraction of 4 mol N m^{-2} over 10.1x11.1 km^2) are included in (Appendix C: ERSEM-BFM model results). An extract from Figure 19 of the area impacted for this scenario is given in Table 7, and similarly for A=50 dm^2/m^2 (annual extraction of 2 mol N m^{-2} over 10.1x11.1 km^2) in Table 6.

Impact percentage	>5%	>10%	>15%	>20%	>25%	>30%	>35%	>40%
Phosphate	0	0	0	0	0	0	0	0
Nitrate	794	0	0	0	0	0	0	0
Ammonium	1792	0	0	0	0	0	0	0
Net Primary Production	1467	235	0	0	0	0	0	0
Gross Secondary Production	118	0	0	0	0	0	0	0
Suspension feeder biomass	<32890**	<6761**	2150	969	217	0	0	0

Table 6. Area impacted [km^2] for given percentages of change for a farm at the Stonehaven site with modelled intensity A=50 dm^2/m^2 over 10.1x11.1 km^2.
**These values are overestimates because they include areas impacted by the effects of the model sensitivity in stratification in the Norwegian Trench.

Impact percentage	>5%	>10%	>15%	>20%	>25%	>30%	>35%	>40%
Phosphate	0	0	0	0	0	0	0	0
Nitrate	5359	564	0	0	0	0	0	0
Ammonium	9796	225	0	0	0	0	0	0
Net Primary Production	2348	110	0	0	0	0	0	0
Gross Secondary Production	0	0	0	0	0	0	0	0
Suspension feeder biomass	<40054**	<9937**	2832	569	217	0	0	0

Table 7. Area impacted [km^2] for given percentages of change for a farm at the Stonehaven site with modelled intensity A=100 dm^2/m^2 over 10.1x11.1 km^2.
**These values are overestimates because they include areas impacted by the effects of the model sensitivity in stratification in the Norwegian Trench.

4.3.4 Significance of the potential impact on the ecosystem

The following definition of significance was suggested:

- define nutrient depletion as a 10% reduction or more
- if nutrient depletion is limited to a distance away from the farm similar to the farm size, then the effects are insignificant
- if nutrient depletion occurs at distances over 100 km away from the operation, then the effects are certainly significant
- for nutrient depletion between these two end-members, local considerations might apply, and the results are considered to be marginally significant

Using this definition of significant impact, and the interpretation and limitations of the model results as discussed above, it is suggested that the effects are expected to be marginally significant. If nutrients were extracted to a level equivalent to the more intensive farming scenarios simulated with the 3D model, then the effects on phytoplankton production would certainly be significant. Our current interpretation, however, is that the results of the lower-intensity farming scenarios simulated with the 3D model are more likely to apply to farming activity as proposed. Further comparison with measured macroalgal C and N contents from field trials, and observed nutrient concentrations of seawater in and around operational kelp farms using the approach of Sanderson et al. (2008) would also be required for full validation. Inclusion of a macroalgae model in the 3D model would be required for a more reliable estimate of whether these levels can be reached with the proposed farming methods/scenarios.

The nitrogen removal associated with seaweed farming may be seen as beneficial in sea areas subject to high loading with anthropogenic nutrients, as this will reverse the eutrophication process. The annual inputs of nitrogen from a major river such as the Clyde are however large (10000-20000 tonnes N yr^{-1}; Nedwell et al. 2002) compared to the 480 tonnes N yr^{-1} uptake capacity of the 20 km^2 kelp farm targeted in our compartment modelling (Figure 21). A farm of this size would remove a broadly similar amount of nitrogen to the 825 tonnes of N currently removed to land each year by the main fishery of the Malin

sea and Minches, for *Nephrops norvegicus* (based on landings of 25000 tonnes fresh weight).

Salmon aquaculture is the major source of anthropogenic nitrogen inputs to the marine environment for the north-west of Scotland, as the riverine input in this low population density region is small (Heath et al. 2002, Rydberg et al. 2003). The farming of salmon at the capacity recorded in 2010 of approximately 150000 tonnes per year releases 7500 tonnes of nitrogen (using feed conversion factors of Davies 2000). Hence, the area of seaweed farm that would be required to cancel the ecological footprint of salmon aquaculture can be calculated as 312 km^2. The nitrogen demand of a 'level 1' seaweed biomass cultivation facility of 560 km^2, as described in the DECC future carbon calculator, would be of greater size than the nitrogen additions due to aquaculture in this region.

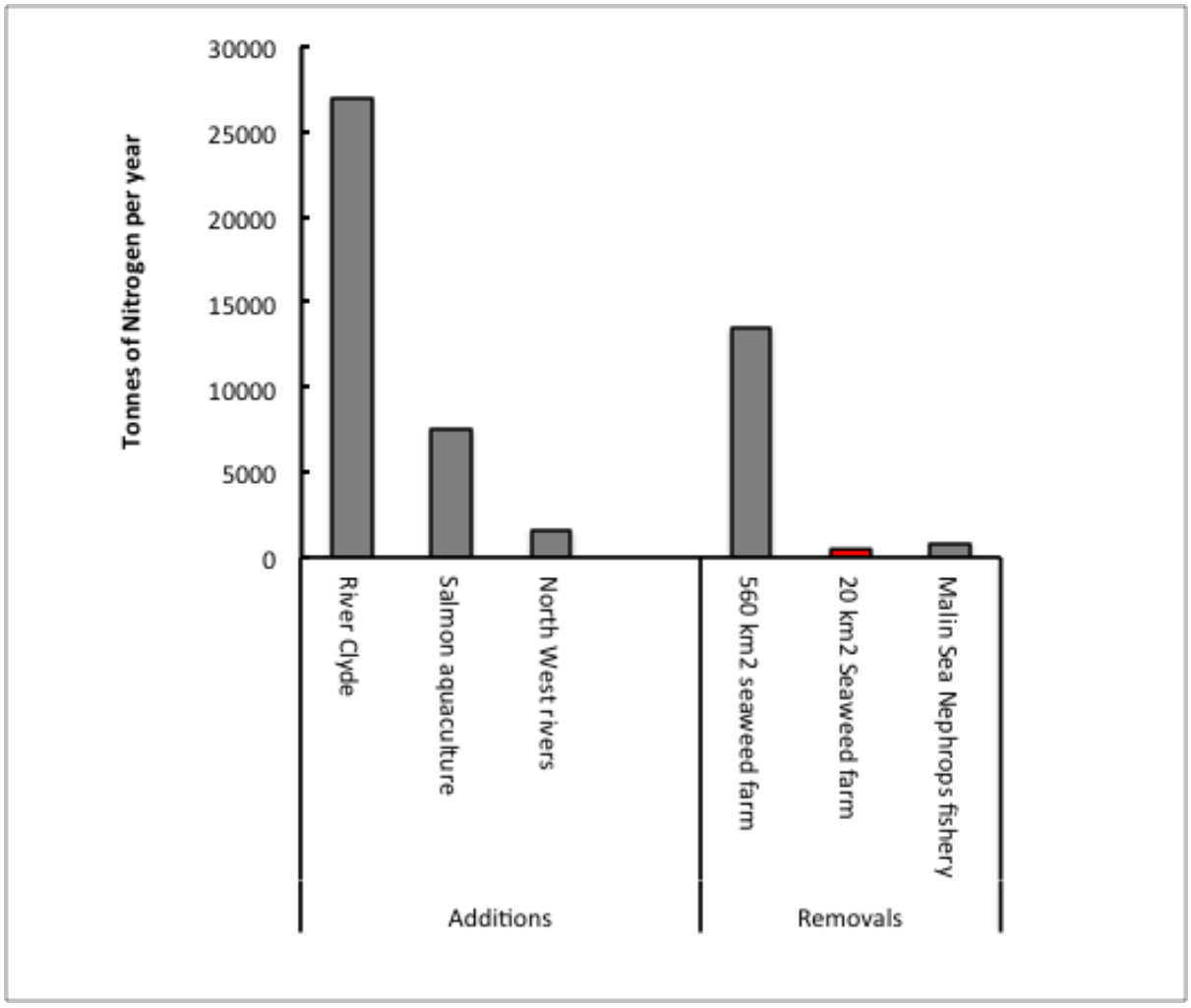

Figure 21: Comparison of selected sources and sinks for nitrogen for the sea area of the west coast of Scotland.

Finally, consideration should be given to the impacts of burst-releases of iodine oxide and other iodocarbons, and precautions taken if necessary to reduce emissions (e.g. avoiding prolonged exposure of harvested kelp material to direct sunlight).

5 Summary

Two model approaches were used to assess the potential environmental impact of hypothetical macroalgae farms: a simple phytoplankton-kelp compartment model and a 3D-coupled hydrodynamics-biogeochemistry model. The CKP model was developed to include a macroalgae growth model, whereas the 3D model was fitted with a nutrient sink to simulate the presence of a macroalgae farm.

The compartment model was able to reproduce the main features of the available growth and chemical composition data for *Saccharina latissima.* The results suggest a very strong reduction in phytoplankton biomass in the vicinity of the production area due to competition for nutrients. These impacts will decrease at larger scales, but are still likely to be greater than 10% with respect to a control (no farm) at distances in excess of 7.5 km from the edge of the production area. The simple spatial structure of the model setup did not allow directionality to be addressed and the distances associated with the predicted impacts were based on a uniform dilution in all directions. Kelp release large quantities of dissolved organic matter as well as continuously shedding fragments of blade material, particularly during the summer. Local deposition of this material near the seabed of a stratified water column will cause enhanced respiration and reduce oxygen concentrations. As with salmon farming, site placement is therefore very important to maximise kelp yields and to dilute waste products.

The GETM-ERSEM-BFM model results, using a nutrient sink to simulate the spatial distribution of effects of a north-east Scotland macroalgal farm on the marine ecosystem

indicated potential reductions in annual-averaged, depth-integrated nutrient concentrations, production and biomass in a strip along the UK east coast up to Norfolk. The magnitude of the changes depended on the variable and on the intensity of the nutrient extraction (farming) imposed, varying from over 40% for the most sensitive variables for the most intensive production of kelp (10.1x11.1 km^2 fully covered with 10 layers of macroalgae thalli) to less than a few percent for non-sensitive variables and/or low-intensity farming (50% of 10.1x11.1 km^2 covered by 1 layer of macroalgae). The far-field effects were not sensitive to the along-shore position of the farm, suggesting a more or less linear cumulative effect in the case of multiple farms. Cross-shore positioning of the farm was not tested. Lookup graphs and tables were constructed for nutrients, primary and secondary production, and filter-feeder biomass for a farm at the Stonehaven site, showing the extent of the area affected by a certain level of change as a function of the nutrient extraction intensity. These might be used to provide a first estimate of potential impact of macroalgae farms in similar settings/conditions. It should be noted that several assumptions were made for the simulations presented in this report (100% removal of nutrients calculated to be taken up by macroalgae; constant, year-round coverage with macro-algae at what may be interpreted as harvest density) that lead to an upper estimate of the effects.

The impacts simulated with the compartment model were smaller both in magnitude and in terms of the size and shape of the area affected than those simulated with the 3D model for equivalent farming intensity *A*. These differences can be traced back to the assumptions made to set up the respective models. Comparison with field data from an experimental farm suggested that the magnitude was probably more accurately predicted by the compartment model, but the shape of the spatial extent of the impact was more accurately predicted by the 3D model. Therefore we expect the results for the lowest-intensity farming scenarios of the 3D model to be most representative of the potential impact of farming activity as proposed. This speculation can be tested by including a macroalgae growth model in the 3D model.

The following definitions were used to assess if the simulated impacts were significant:

- define nutrient depletion as a 10% reduction or more
- if nutrient depletion is limited to a distance from the farm similar to the farm size, then the effects are insignificant
- if nutrient depletion occurs at distances over 100 km away from the operation, then the effects are certainly significant
- for nutrient depletion between these two thresholds, local considerations might apply, and the results are considered to be marginally significant

We conclude that, given these definitions and based on the model simulations, the effects of the proposed farming activity on nutrient concentrations are not expected to be 'insignificant' in terms of the definitions given in the discussion, but more likely 'marginally significant'. Given a sufficiently high level of farming activity (combination of intensity and size of the farm(s)), the effects might become 'certainly significant'. Improved models, and specific setups and simulations for actually planned scenarios are recommended to provide better estimates ok kelp production and its impacts on water quality and local ecosystems.
The effects of nutrient removal would be the reverse of the symptoms of eutrophication i.e. a lower nutrient concentration in the water, decreased productivity and energy fluxes through the pelagic system, decreased flux of organic material to the seabed, and subtle alteration to community structure. These changes would occur in the long term against a background of considerable natural variability in the exchange of UK shelf seas with the open ocean, which is one of the main controls on nutrient availability (Holt et al. 2012). For example, winter nutrient values from the Stonehaven time series site show a standard deviation of 2.0 umol nitrate l^{-1} which is 26% of the long-term mean of 7.7 umol nitrate l^{-1}. To determine actual changes in any ecosystem parameters would require the set-up of a dedicated monitoring programme.

6 Recommendations

General recommendations:

- Cumulative effects of multiple farms should be investigated, both in terms of environmental impact and of inter-farm impact on performance.
- Interactions with other existing and planned large-scale human activities (wind farms, wave farms, tidal energy farms) should be investigated, both in terms of economic performance and combined environmental impact.
- Observations in the field of annual budgets of nutrients taken up by macroalgae would be useful in order to validate the models.

7 References

Abdullah, M. I., Fredriksen, S. (2004). Production, respiration and exudation of dissolved organic matter by the kelp *Laminaria hyperborea* along the west coast of Norway. Journal of the Marine Biological Association of the UK, 84(5): 887-894.

Aldridge, J. (2005) An Assessment of Nutrient Dynamics and Green Seaweed Growth in the Medway Estuary. Report prepared for the EA

Aldridge J.N., Tett, P., Painting, S.J., Capuzzo, E., Mills, D.K. (2010). The dynamic Combined Phytoplankton and Macroalgae (CPM) Model: Technical Report. Contract C3290 Report, Environment Agency.

Baretta, J.W., Ebenhöh, W., Ruardij, P. (1995). The European Regional Seas Ecosystem Model, a complex marine ecosystem model. Netherlands Journal of Sea Research 33: 233-246.

Baxter, J. M., I. L. Boyd, M. Cox, A. E. Donald, S. J. Malcolm, H. Miles, B. Miller, and C. F. Moffat. 2011. Scotland's Marine Atlas: Information for the national marine plan.

Bouwman, A.F., Pawlowski, M., Liu, C., Beusen, A.H.W., Shumway, S.E., Glibert, P.M., Overbeek, C.C., 2011b. Global Hindcasts and Future Projections of Coastal Nitrogen and Phosphorus Loads Due to Shellfish and Seaweed Aquaculture. Reviews in Fisheries Science 19, 331-357.

Broch, O.J., Slagstad, D. (2011). Modelling seasonal growth and composition of the kelp *Saccharina latissima*. Journal of Applied Phycology 173527.

Carpenter, L.J., Liss, P.S. (2000). On temperate sources of bromoform and other reactive organic bromine gases. Journal of Geophysical Research 105(D16): 20,539–20,548.

Cefas (2012). The wider environmental effects of large-scale macroalgal cultivation in Scotland: literature review and model development. Cefas contract C5567 contract for The Crown Estate.

Drew, E.A. (1983). Physiology of *Laminaria*. Seasonal variation of photosynthesis and respiration in *Laminaria digitata* LAMOUR, *L. hyperborea* (GUNN.) FOSL. and *L. saccharina*,

(L.) LAMOUR. and a model for calculation of annual carbon budgets. Marine Ecology 4(3): 227-250.

Dring, M.J. (2012), enAlgae presentation at http://www.enalgae.eu/presentations.html)

Engel, A. (2000). The role of transparent exopolymer particles (TEP) in the increase in apparent particle stickiness (α) during the decline of a diatom bloom. Journal of Plankton Research 22(3): 485-497.

Espinoza, J., Chapman, A.R.O (1983) Ecotypic differentiation of *Laminaria longicruris* in relation to seawater nitrate concentration. Marine Biology: 74, 213-218

Gillibrand, P.A., Sammes, P.J., Slesser, G., Adams, R.D. (2003). Seasonal water column characteristics in the little and north Minches and the Sea of the Hebrides. I. Physical and chemical parameters. Fisheries Research Services Internal Report No 08/03, FRS Marine Laboratory, Aberdeen, 40 pp.

Gordillo, F.J.L., Aguilera, J., Jiménez, C. (2006). The response of nutrient assimilation and biochemical composition of Arctic seaweeds to a nutrient input in summer. Journal of Experimental Botany 57(11): 2661-71.

Heath, M. R., A. C. Edwards, J. Patsch, Turrell, W. R. (2002). Modelling the behaviour of nutrient in the coastal waters of Scotland, Fisheries Research Service Report 10/02.

Herman, P.M.J., Middelburg, J.J., van de Koppel, J., Heip, C.H.R. (1999). Ecology of estuarine macrobenthos. Advances in Ecological Research 29: 195-240.

Christopher J. Hulatt C.J., Thomas, D.N., Bowers,D.G. Norman,L., Zhang, C. (2009) Exudation and decomposition of chromophoric dissolved organic matter (CDOM) from some temperate macroalgae. Estuarine, Coastal and Shelf Science 84: 147-153

Kelly, Dworjanyn (2008). The potential of marine biomass for anaerobic biogas production. The Crown Estate, 103 pages, ISBN: 978-1-906410-05-6.

Küpper, F.C., Carpenter, L.J., McFiggans, G.B., Palmer, C.J., Waite, T.J., Boneberg, E.-M., Woitsch, S., et al. (2008). Iodide accumulation provides kelp with an inorganic antioxidant impacting atmospheric chemistry. Proceedings of the National Academy of Sciences of the United States of America 105(19): 6954-8.

Leigh, R.J., Ball, S.M., Whitehead, J., Leblanc, C., Shillings, A.J.L., Mahajan, A.S., Oetjen, H., et al. (2010). Measurements and modelling of molecular iodine emission, transport and

photodestruction in the coastal region around Roscoff. Atmospheric Chemistry and Physics 10(23): 11823-11838.

Lenhart, H.J., Mills, D.K., Baretta-Bekker, H., van Leeuwen, S.M., van der Molen, J., Baretta, J.W., Blaas, M., Desmit, X., Kühn, W., Lacroix, G., Los, H.J., Ménesguen, A., Neves, R., Proctor, R., Ruardij, P., Skogen, M.D., Vanhoutte-Grunier, A., Villars, M.T., Wakelin, S.L. (2010). Predicting the consequences of nutrient reduction on the eutrophication status of the North Sea. Journal of Marine Systems 81: 148-170.

Lüning, K. (1969). Standing crop and leaf area index of the sublittoral *Laminaria* species near Helgoland. Marine Biology 3(3): 282-286.

Lüning K. (1979). Growth strategies of three *Laminaria* species (Phaeophyceae) inhabiting different depth zones in the sublittoral region of Helgoland (North Sea). Marine Ecology - Progress Series 1, p. 195-207.

Lüning, K. (1990). Seaweeds. Their environment, biogeography and ecophysiology. London: Wiley Interscience.

Lüning, K., Pang, S. (2003). Mass cultivation of seaweeds: current aspects and approaches. Journal of Applied Phycology 15(2/3): 115-119.

Manley S.L., Dastoor, M.N. (1988), Methyl iodide (CH3I) production by kelp and associated microbes. Marine Biology 98:477-482

Matthews, V., Buchholz, F., Saborowski, R., Tarling, G.A., Dallot, S., Labat, J.P. (1999). On the physical oceanography of the Kattegat and Clyde Sea area, 1996–98, as background to ecophysiological studies on the planktonic crustacean, *Meganyctiphanes norvegica* (Euphausiacea). Helgoland Marine Research 53: 70–84.

Nitschke, U., Ruth, A.A., Dixneuf, S., Stengel, D.B. (2011). Molecular iodine emission rates and photosynthetic performance of different thallus parts of *Laminaria digitata* (Phaeophyceae) during emersion. Planta 233(4): 737-48.

Peperzak, L., Colijn, F., Gieskes, W.W.C., Peeters, J.C.H. (1998). Development of the diatom-*Phaeocystis* spring bloom in the Dutch coastal zone of the North Sea: the silicon depletion versus the daily irradiance threshold hypothesis. Journal of Plankton Research 20(3): 517-537.

Peteiro, C., Freire, Ó. (2011). Effect of water motion on the cultivation of the commercial seaweed *Undaria pinnatifida* in a coastal bay of Galicia, Northwest Spain. Aquaculture 314(1-4): 269-276.

Radach, G., Moll, A. (2006). Review of three-dimensional ecological modelling related to the North Sea shelf system. Part II: Model validation and data needs. Oceanography and Marine Biology: An Annual Review 44: 1-60.

Reith (2009) Presentation to Seaweed Bioenergy Research Forum (http://www.supergen-bioenergy.net/Resources/user/docs/new/)

Rippeth, T.P., Jones, K.J. (1997). The seasonal cycle of nitrate in the Clyde Sea. Journal of Marine Systems 12(1-4): 299-310.

Ruardij, P., van Haren, H., Ridderinkhof, H. (1997). The impact of thermal stratification on phytoplankton and nutrient dynamics in shelf seas: a model study. Journal of Sea Research 38: 311-331.

Ruardij, P., van Raaphorst, W. (1995). Benthic nutrient regeneration in the ERSEM-BFM ecosystem model of the North Sea. Netherland Journal of Sea Research 33: 453-483.

Ruardij, P., Veldhuis, M.J.W., Brussaard, C.P.D. (2005). Modeling the bloom dynamics of the polymorphic phytoplankter *Phaeocystis globosa:* impact of grazers and viruses. Harmful Algae 4: 941-963.

Rydberg, L., B. Sjöberg, and A. Stigebrandt. 2003. The Interaction between Fish Farming and Algal Communities of the Scottish Waters - a Review. Scottish Executive Research Report 2003-04.

Sanderson, J.C., Cromey, C.J., Dring, M.J., Kelly, M.S. (2008). Distribution of nutrients for seaweed cultivation around salmon cages at farm sites in north–west Scotland. Aquaculture 278(1-4): 60-68.

Sjøtun, K. (1993). Seasonal lamina growth in two age groups of *Laminaria saccharina* (L.) Lamour in Western Norway. Botanica Marina 36: 433-441.

Slesser, G., Turrell, W.R. (2005). Annual cycles of physical chemical and biological parameters in Scottish waters (2005 update). Fisheries Research Service, Internal Report 19/05.

Solidoro, C., Pecenik, G., Pastres, R., Franco, D., Dejak, C. (1997). Modelling macroalgae (*Ulva rigida)* in the Venice Lagoon: Model structure identification and first parameter

estimation. Ecological Modelling 94: 191-206.

Steen, H. (2009). Chapter 2.11. Stortare. Kyst og havbruk. Institute of Marine Research.

Tett, P. (1990). The photic zone. In: Herring, P., Campbell, A., Whitfield, M., Maddock, L. (Eds.). Light and Life in the Sea. Cambridge University Press, Cambridge, U.K.: 59–87.

Tett, P. (1998). Parameterising a microplankton model. Napier University, Edinburgh, report.

Tett, P., Gilpin, L., Svendsen, H., Erlandsson, C.P., Larsson, U., Kratzer, S., Fouilland, E., Janzen, C., Lee, J-Y., Grenz, C., Newton, A., Ferreira, J.G., Fernandes, T., Scory, S. (2003). Eutrophication and some European waters of restricted exchange. Continental Shelf Research 23: 1635–1671.

Tett, P., Portilla, E., Gillibrand, P., Inall, M., (2011). Carrying and assimilative capacities: the ACExR-LESV model for sea-loch aquaculture. Aquaculture Research 4: 1365-2109.

Tett, P., Wilson, H. (2000). From biogeochemical to ecological models of marine microplankton. Journal of Marine Systems 25(3-4): 431-446.

Turrell, W. R., G. Slesser, R. Payne, R. D. Adams, and P. A. Gillibrand. 1996. Hydrography of the East Shetland Basin in relation to decadal North Sea variability. ICES Journal of Marine Science 53: 899–916.

Vichi, M., May, W., Navarra, A. (2003). Response of a complex ecosystem model of the northern Adriatic Sea to a regional climate change scenario. Climate Research 24: 141-158.

Vichi, M., Pinardi, N., Masina, S. (2007). A generalized model of pelagic biogeochemistry for the global ocean ecosystem. Part I: Theory. Journal of Marine Systems 64: 89-109.

Vichi, M., Ruardij, P., Baretta, J.W. (2004). Link or sink: a modelling interpretation of the open Baltic biogeochemistry. Biogeoscience 1: 79-100.

Wada, S., Aoki, M.N., Tsuchiya, Y., Sato, T., Shinagawa, H., Hama, T. (2007). Quantitative and qualitative analyses of dissolved organic matter released from *Ecklonia cava* Kjellman, in Oura Bay, Shimoda, Izu Peninsula, Japan. Journal of Experimental Marine Biology and Ecology 349(2): 344-358.

Walker, F.T. (1954) Distribution of Laminariaceae around Scotland. J. Conseil.20: 160-164

Whitehead, J.D., McFiggans, G.B., Gallagher, M.W., Flynn, M.J. (2009). Direct linkage between tidally driven coastal ozone deposition fluxes, particle emission fluxes, and subsequent CCN formation. Geophysical Research Letters 36(4): L04806.

8 Appendix A: CKP model description

This section gives a technical description of the macroalgal model. The Combined Phytoplankton and Macroalgae (CKP) model can be used to predict the biomass of phytoplankton and macroalgae-type communities in generic water bodies. The key model outputs are estimates of dissolved nitrate concentrations (mmol m^{-3}), phytoplankton chlorophyll concentrations (mg chl m^{-3}) and macroalgae frond area per surface area of the domain (dm^2 m^{-2}). The macroalgal sub-model closely follows the model of Broch & Slagstad (2011). Although the processes modelled are applicable to wide number of macroalgal species, the particular model here has been calibrated and designed to describe the kelp *Saccharina latissima*.

8.1 State variables

Model predictions are made for the following:

A - average macroalgae area per surface area of density (dm^2 m^{-2})

Q - Internal nitrogen (mmol N dm^{-2})

C - Internal carbon (g C dm^{-2})

N - external dissolved nitrogen concentration (uM).

X - average phytoplankton represented as chlorophyll (mg l^{-1})

Forcing parameters are water temperature T (^oC) and illumination I (µmol photons m^{-2} s^{-1}).

8.2 Spatial coupling

The model can link together a number of compartments of given volume with nutrients and phytoplankton exchange occurring between adjacent compartments. Consider a set of three nested regions with volumes V_1, V_2, V_3 as shown in Figure 22 with the outer region connected to an assumed infinite exterior l region (region zero) with a specified nutrient and chlorophyll concentration. Let C_i be any property (e.g. nutrient concentration) in compartment *i* and let v_{ij} (m^3d^{-1}) be the volume exchange per unit time between region i and j, then the following equations are used to model the conservative transport of C between model compartments (here 3 compartments are considered, but the number can be arbitrary)

$$\frac{d}{dt}(C_1V_1) = B_1 - v_{12}(C_1 - C_2) + v_{01}(C_0 - C_1)$$
$$\frac{d}{dt}(C_2V_2) = B_2 - v_{23}(C_2 - C_3) + v_{12}(C_1 - C_2)$$
$$\frac{d}{dt}(C_3V_3) = B_3 + v_{23}(C_2 - C_3)$$

where the B_i represent all other processes (source inputs or biological interactions) occurring in the compartment. If A_{ij} is the surface area connecting compartment i to j then the volume fluxes are assumed to parameterised as $v_{ij} = u\ A_{ij}$ where u is a fixed quantity with units of velocity that represents in a generic way the scale of mixing in the region.

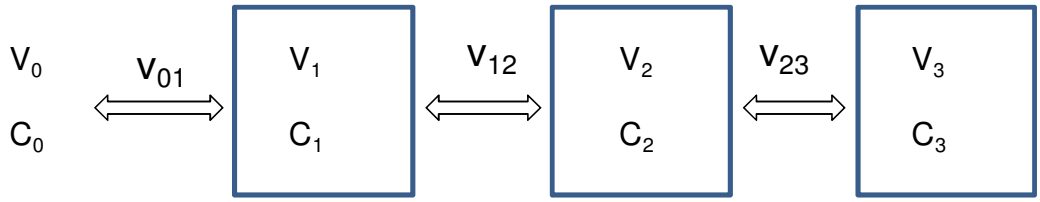

Figure 22: Example compartment arrangements and connections.

8.3 Macroalgae model

The key state variable is projected frond area per m^{-2} of surface area of the domain. Two further key state variables are the amount of internal nitrogen per frond area Q (mmol N dm^{-2}), and the amount of carbon per frond area C (g C dm^{-2}). This is assumed to consist of a structural component and a stored component. Observations suggest a minimal nitrogen and carbon level as a percentage of dry weight (assumed to be convertible to a value per frond area). The minimum value is taken to be structural and any value in excess of this assumed to represent a stored form. For carbon this takes the form of the carbohydrates mannitol and laminaran. Note we deviate from the formulation of Broch & Slagstad (2011) who introduce separate structural and minimum values.

Many biological processes dependent on a quantity X exhibit behaviour where the process rate increases approximately linear dependence at small values of X but saturate as values approach a measured value k_x and saturate to a fixed value of one as $x >> k_x$.(see Figure 23). This is often modelled using a function of the form.

$$m(X;k_x) = X/(X+k_x)$$

where k_X is the half saturation constant for X. In different biogeochemical l contexts the relationship goes by the name 'Monad' form, Holling type II or Michaelis-Menten dynamics. We use this functional relationship extensively in the model formulation.

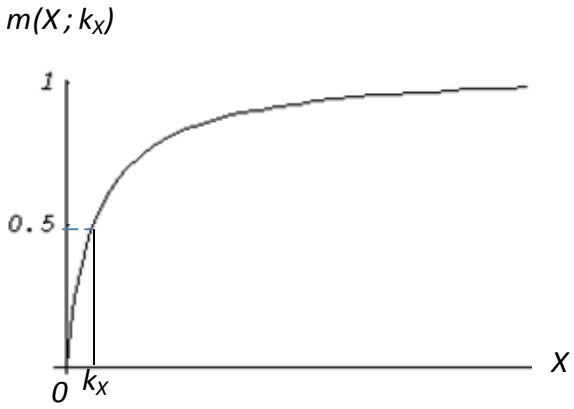

Figure 23: Saturated behaviour (Monad form).

8.3.1 Nutrient uptake and storage

The equations for nitrogen uptake and internal storage with density Q (mmol N dm^{-2}) and the corresponding loss term from the external nutrient concentration N (mmol m^{-3}) in a compartment with water depth *h* are

$$\frac{dQ}{dt} = (\Psi_N^* - \mu_A)Q \qquad (1)$$

$$\frac{dN}{dt} = -\Psi_N A/h \qquad (2)$$

Note in equation (2) the biomass per unit area A is divided by the water depth *h* to convert from units of area to units of volume. The last term μ_A in equation (1) is the growth rate the form of which is given later. Uptake of nitrogen from the water is modelled as

$$\Psi_N^* = \Psi_N / Q \qquad (3)$$

$$\Psi_N = V_{\max} \times m(N; k_N) \times (Q_{\max} - Q)/(Q_{\max} - Q_{\min}) \qquad (4)$$

where V_{max} (mmol N dm^{-2} d^{-1}) is the maximum experimentally observed uptake rate and where the limiter functions inhibit uptake when external nitrogen N is low (of order of k_N) or the internal nitrogen Q approaches the specified maximum storage capacity Q_{max}.

8.3.2 Carbon uptake and storage

The equation for internal carbon storage C density (g C dm^{-2}), is

$$\frac{dC}{dt} = \Psi_C - \tilde{\mu}_A \, C \qquad (5)$$

The net photosynthetic production modelled as

$$\Psi_C = P(I,T) \times [1 - E(C)] - R(T)$$

where *P (I)* is the gross photosynthetic production rate (g C dm^{-2} d^{-1}), R (T) is the respiration rate and E(C) is the proportion of photosynthetically produced carbon that is exuded. The latter occurs as internal carbon approaches the limits of storage leading to excess carbon photosynthesis are released into the water as carbohydrates.

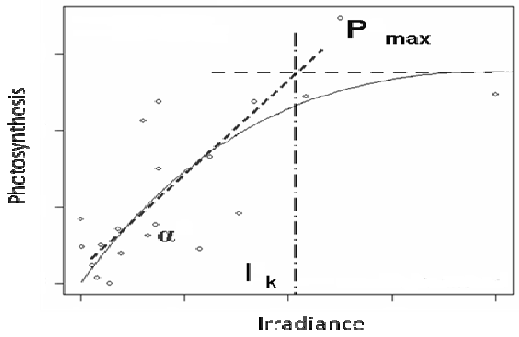

Figure 24: Piecewise linear photosynthetic rate.

The formulation in the model assumes photosynthetic production at a given instant is given by a piecewise linear curve that includes the effect of saturation (Figure 24)

$$P(t) = \alpha \times \min\{ I(t), I_k \}$$

where α (g C dm^{-2} h^{-1} (umol photon m^{-2} s^{-1})$^{-1}$) is the photosynthetic efficiency, I_k (µmol photon m^{-2} s^{-1}) is the light saturation point and I (t) (µmol photon m^{-2} s^{-1}) is the hourly average light intensity. Both α and I_k are species specific. The macroalgae frond is assumed to lie flat at given depth (although it may flip over) and only the projected surface area is taken account of when calculating production. The light intensity at depth *h* (m) is

$$I(t) = I_0(t) \, Exp(-k_d \, h)$$

where I_0 is the surface incident value and k_d is the water column attenuation coefficient. If tidal variation in depth is being considered then h can include the tidal elevation. Self shading is not considered taken into account. If for a given day *I (t)* is the variation in photon

flux over a 24 hour period experienced by the macroalgae then the species specific total daily saturation corrected photon flux is calculated as

$$\hat{I} = \int_0^{24} \min\{ I(t), I_k \}\, dt$$

from which the total daily carbon production (g C dm^{-2} d^{-1}) is given by $P(\hat{I}) = \alpha \hat{I}$.

The daily light curve for the surface illumination $I_0\ (t)$ is modelled as the product of the daily mean value (a function of latitude, time of year and cloud cover) and a Gaussian diurnal variation

$$I_0(t) = \bar{I} \times I_d(t)$$
$$I_d(t) = A\ \exp\{-[3.45\,(t-12)/\sigma]^2\}$$

where t is measured in hours since midnight and the width of the Gaussian curve is controlled by the day length d with $\sigma = 0.31d$. Day length is calculated as a function of latitude and the time of year using a standard expression (ref). The normalisation constant A is defined such that integrated over T=24 hours, the average value of I_d is unity.

Respiration is generally considered to be temperature dependent although observations do not always show strong evidence for this (Drew, 1983). For simplicity a constant value respiration rate R_0 was assumed in the model. To prevent stored carbon dropping below minimum value, respiration is allowed to decrease as carbon reserves approach their minimum value using a Monad saturation function with small half-saturation constant δ_{RC}

$$R(C) = R_0 \times m(C - C_{\min}; \delta_{RC})$$

Exudation is assumed to occur when high concentrations of stored carbohydrates build up. Little is known of this process and the modelling of this process is tentative. Following Broch & Slagstad (2011) an exponentially increasing exudation rate as a function of carbon content of the form $E1(C) = 1 - \exp[\gamma(C - C_{\min})]$

is used, where γ is an empirical constant.

8.3.3 Macroalgae growth

The standard formulation for macroalgae (e.g. Broch & Slagstad 2011, Solidoro 1997, Aldridge 2005) adopted from phytoplankton and modelling of green Ulva type seaweeds is to assume rate of biomass increase is proportional to the existing biomass at a given instant. Using area A as a measure of biomass this is a relationship of the form $dA/dt = \mu_A A$, implying exponential growth for constant growth rate μ_A. However for kelp species at least, growth of new tissue typically occurs at the base of the frond and it is not clear the size of this area will scale the overall frond area as implied by the exponential growth law. Certainly observations of growth tend to be reported as increase in length, or area, per unit time rather than as a specific growth rate μ_A (units of inverse time). Thus it might be better to model growth with a relation of the form $dA/dt = \mu$ form (implying linear growth over time for constant μ). Although this is an important difference in the basic model approach, in practice it probably will not make a fundamental difference once the model has been appropriately calibrated with observation information. This is because μ is not constant but depends strongly on the coupling with nutrient and carbohydrate availability as well as temperature and other factors and this behaviour dominates the overall growth predictions. In fact both approaches are only an approximation and it seems likely that a satisfactory model can be developed using either. In this study we adopt the standard approach and assume a growth rate at any given time is proportional to the existing biomass. Similar arguments can be made about the loss term but again we adopt a conventional formulation and assume the loss rate will increase with frond area. Thus net growth of macroalgae frond area will be a balance between growth and loss that is modelled in the form

$$\frac{dA}{dt} = (\mu_A - \lambda_A)A \qquad (6)$$

The growth and loss rate functions are given by

$$\mu_A = \mu_{\max}^{(A)} \times f_T \times f_{day} \times \min\{f_Q, f_C\}$$

$$\lambda_A = \lambda_0(t) \times m(A - A_{\min}; \delta_A)$$

where $\mu_{\max}^{(A)}$ (units d^{-1}) is the maximum macroalgae growth rate and f_T, f_{day} are limiter functions. The loss rate is a product of a time dependent term and a factor that prevents the area falling below a specified minimum value.

Following Broch & Slagstad (2011) limitation on growth due to internal nutrient and carbohydrate concentrations are given by

$$f_Q = 1 - Q_{\min}/Q$$
$$f_C = 1 - C_{\min}/C$$

A temperature modification to growth is parameterised as in Broch & Slagstad (2009) (Figure 25) with optimal growth between 10 and 15°C and zero growth above 19 °C. This can be represented in functional form as

$$\mathrm{f_T} = \max\{0, \min\{1, \{2\mathrm{T}+5)/25\}\} - \max\{0, \min\{1, (\mathrm{T}-15)/4\}\}$$

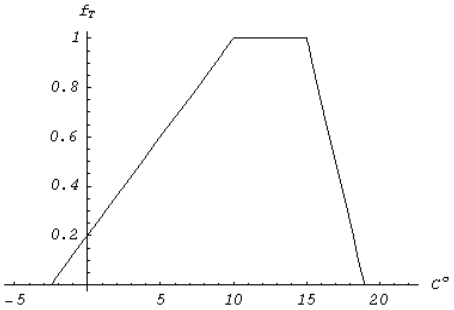

Figure 25: Temperature adjustment of growth rate.

A limiter function equivalent to f_{day} was introduced by Broch & Slagstad (2011) in order to fit observed growth characteristics, in particular the measurements of Sjøtun (1993). At present the form has no strong biological basis but nevertheless it (or something analogous) appears necessary to reproduce the observed growth behaviour in October to December. The need arises because by early winter both internal and external nutrient concentrations carbohydrates reserves built up over summer and are relatively high. Thus renewed growth from November through December appears possible and, in the model, is

predicted. However the observations of Sjøtun (1993) appear to show significant growth starting only in January suggesting that some mechanism is inhibiting growth before that. To model this, the limiter function f_{day} (f_{photo} in Broch & Slagstad, 2011) is introduced dependent on the rate of change of day length. This quantity switches from negative to positive at midwinter and f_{day} is constructed to inhibit growth while day length is decreasing. The functional form used is as given as in Broch & Slagstad (2011)

$$f_{day}(t) = a_2 + a_1[1 + \mathrm{sgn}(\Delta L(t))\,|\Delta L(t)|^{1/2}]$$

where ΔL is the normalised change of day length per day ($-1 \le \Delta L \le 1$) with the extreme of the range occurring at the equinoxes and a_1 and a_2 are fitting constants.

The rate of frond area loss is the modelled as the product of a time dependent specific rate and a limiter function preventing the plant area dropping below a minimum value A_{mi} on the assumption that over a compete annual growth cycle the plant does not decrease in size. This is implemented using a using a Monad saturation function with small half-saturation constant δ_A,

$$\lambda_A = \lambda_0(t) \times m(A - A_{\min}; \delta_A)$$

The time dependent loss rate can used to reflect seasonal effects such as summer predation or the effect of wave action due to winter storms.

8.3.4 Derived quantities

The key state variable is A, projected frond area per m^{-2} of surface area of the domain. Two weights (g m^{-2}) can be derived from this: structural, dry and wet weights notated as w_s, w_d and w_w respectively with $w_s \le w_d < w_w$. The structural weight is the dry weight of the plant minus the stored carbon and nutrient reserves. The dry weight is structural weight plus reserve carbohydrates and nutrients and wet (or fresh) weight includes in addition the water content. As in Broch & Slagstad (2011) it was assumed that

frond area can be directly related to the 'structural' weight with constant of proportionality k_A (g dm^{-2}) such that

$$w_s = k_A A$$

The concept of structural weight is avoided in the model formulation but the conversion factor is necessary when converting units derived from Broch & Slagstad (2011) into per frond area values. Also derived from Broch & Slagstad (2011) is the conversion from frond area to dry and wet weights, taking account of the weight of the stored carbohydrate and nitrate reserves. The model predicts carbon weight, however a given weight of carbon stored as carbohydrate is associated with additional hydrogen and oxygen atoms and a conversion factor from carbon to the associated total weight is needed to compare with observed dry weights. Assuming the known storage molecules (laminaran, mannitol and alginate) occur in fixed the relative proportions a conversion factor k_C (g dw (g C)$^{-1}$) was derived by Broch & Slagstad (2011). A similar procedure yields k_N (g dw (g N)$^{-1}$) that converts from modelled stored nitrogen concentration to dry weight by making assumptions about the molecular composition of the nitrogen storage. Dry weight is then calculated from

$$w_s = [k_A + k_C (C - C_{\min}) + k_N (N - N_{\min})]A$$

Wet weight is not used in this study so a conversion formula is not presented.

Within the inner compartment of the model an average macroalgal density per square metre is assumed. The CKP does not distinguish between a lower density of plants arranged evenly over the whole compartment (e.g. growth on a net), or a higher density confined to a more restricted sub-region (e.g. growth on ropes or lines).

8.4 Phytoplankton model

The (micro) phytoplankton sub-model is essentially that described in detail in a series of publications by Tett et al. and only a summary description is given here. Phytoplankton biomass is represented as chlorophyll concentration X (mg chl m^{-3}). In contrast to the macroalgae phytoplankton growth is modelled assuming nutrient and carbon uptake rates are proportional to the phytoplankton growth rate and the internal ratio of nutrient content to biomass is specified with a fixed average value. With these assumptions uptake and

growth can be combined into a one stage process and phytoplankton growth and the corresponding dissolved nitrate balance are then

$$\frac{dX}{dt} = (\mu_X - \lambda_X) X - E \qquad (7)$$

$$\frac{dN}{dt} = -\mu_X \; X \, Q_X - E$$

where E is the exchange with surrounding regions, Q_X (mmol N (mg chl)$^{-1}$) is a fixed quotient of internal nitrate normalised to chlorophyll and

$$\mu_X = g_{1T} \times \min\{\mu_N, \mu_I\}$$
$$\lambda_X = g_{2T} \times L$$

Here the $g_{1,\,2T}$ are temperature dependent modifiers modelled using a standard 'Q_{10}' formulation

$$g_T = Q_{10} \exp[-(T - T_{ref})/10]$$

The nutrient and light controlled growth rates are respectively

$$\mu_N = \mu_{\max}^{(X)} \times m(N; k_N)$$
$$\mu_I = \alpha^{(X)} (\hat{I} - I_c)$$

where μ_{max} (d^{-1}) is the maximum nutrient related growth rate, $\alpha^{(X)}$ (d^{-1} (umol photon m^{-2} s^{-1})$^{-1}$) is the effective photosynthetic efficiency normalised to chlorophyll, and I_c (umol photon m^{-2} s^{-1}) is a compensation irradiance (Tett, 1990). As described in Tett (1998), Tett et al. (2003), these parameters are effective values calculated assuming the plankton consists of a mixture of autotrophic and 'fast' micro-heterotrophic processes. The values of the effective plankton parameters are calculated from a larger set of 'primitive' micro-algal and micro-heterotrophic parameters and combined using a heterotroph fraction parameter that is the ratio of micro-heterotroph (carbon) biomass to the total biomass of the (micro)plankton (Tett & Wilson, 2000). The value of this parameter can be set to model either a diatom like phytoplankton population (early spring growth) or flagellate like ones (later growth) or some combination of the two.

8.5 Dissolved nutrient model

Combining the loss terms from macroalgal and phytoplankton growth and including nutrient regeneration terms the equation for dissolved nitrogen concentration (mmol N m^{-3}) is

$$\frac{dN}{dt} = -(\Psi_N^* - e_A \lambda_A) Q A / h - (\mu_X - e_X \lambda_X) Q_x X - E \qquad (8)$$

where E represents exchange with surrounding compartments. In the above a fixed fraction 'e' of the phytoplankton and macroalgae loss rate flux is assumed to be instantaneously remineralised and returned to the nutrient pool. Both phytoplankton and macroalgae are subject to loss terms representing zooplankton grazing and frond erosion respectively. For phytoplankton it was assumed that 50% of the nutrients associated with lost biomass were instantaneously regenerated and returned to the external nutrient pool for reuse. For macroalgae it was assumed that the nutrients were less readily returned and 25% of nutrients due to frond loss were recycled back into the water column. There is little data at the moment to verify this number which will depend also on local conditions.

8.6 Initial values

The initial macroalgae area density plays an important role in determining the maximum subsequent growth and it is where the role of the area assumed to be cultivated and the packing density within it come in. The model cannot distinguish between at scales below that of the compartment area. If we have ρ_p plants per m^{-2} with average frond area a_0 (dm^2) at the start of the growing season and the proportion of the model area domain area cultivated is ϑ the initial frond area density (dm^2 m^{-2}) is

$A(0) = \rho_p \vartheta a_0$

Assuming the model starts in January the following assignments are made for the other state variables

$Q(0) = Q_{max}$

$C(0) = C_{min}$

$X(0) = X_{winter}$

8.7 Calibration of macroalgal sub-model

This section describes the assignment of model parameters based on measurements reported in the literature together with a calibration exercise using the data of Sjøtun (1993). Different field and laboratory investigations often report rather different values for many of the parameters of interest and collectively the outputs from these studies can best be regarded as guides to the acceptable range of a parameter rather than supplying a single definitive value.

In assigning parameter values there is a general issue because of the variety of units that have been used in the literature to report measurements. Additional assumptions are required to convert values to a consistent set required for modelling. A particular issue arises with parameters that are reported per unit dry weight of kelp. Dry weight is best regarded as a derived variable that depends on both the plant size (expressed as area) and the amount of stored carbohydrates, with the ratio between dry weight and area showing a pronounced seasonal variation (ranging from 0.5 to 2) dependent on the carbohydrate reserves. For the model, values expressed per unit dry weight were converted to values per (frond) area (dm^{-2}) using a conversion factor k_A =0.6 g dw dm^{-2} as used by Broch & Slagstad (2011).

For the kelp sub-model a review of literature indicated that the data of Sjøtun (1993) provided the most comprehensive set of measurements available in that it included values for most of the forcing and state variables required for model calibration. The results reported in Sjøtun (1993) are based on an average of around 70 specimens of a natural population with a mixture of plants in their 2^{nd} and 3^{rd} year of growth. It is noted that the population of kelp studied by Sjøtun (1993) was on the Norwegian rather than Scottish coast. Broch & Slagstad (2010) whose model served as the basis for the model developed in this study also used this data set to develop calibrate their model.

Some additional processing of the published data of Sjøtun (1993) was undertaken to convert growth rates expressed as *length per day* to *area per day*. This was done using the reported frond width measurements for newly grown material and taking the product of

this with the rate of increase of length to give the rate of area increase. Similarly width estimates were required to reconstruct the area loss rates from the loss of frond length reported. This was subject to potentially larger errors because the average width of the lost material was not given directly but had to be inferred by relating the age of the lost tissue back to the width it would have been when newly grown, assuming this width did not changed as the tissue aged.

The nitrate conditions measured by Sjøtun (1993) showed a winter peak of approximately 7 mmol m^{-3} reducing to effectively zero by the end of April then increasing from October to recover to peak values in January (Figure 26a). The model was started in January with initial nitrate concentrations set to match the Sjøtun (1993) measurements. Phytoplankton behaviour can be controlled in the model by the value of the heterotrophy parameter (Appendix A), with early spring bloom associated with lower value of this ratio representing a more diatom -like phytoplankton behaviour. The kelp sub-model was run coupled with the phytoplankton model with the heterotroph ratio was set to yield an April phytoplankton spring bloom leading to dissolved nitrate concentrations being effectively zero by the end of April in agreement with the measurements of Sjøtun (1993). Nutrients were replenished in the period from September to mid February simulating an autumn/winter recovery in concentrations that comes from remineralisation of detrital material and renewal by oceanic water.

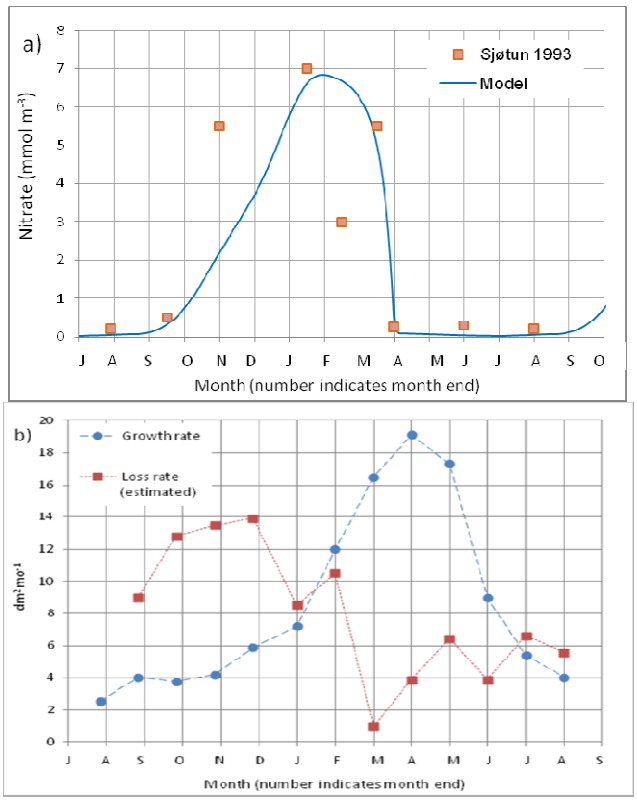

Figure 26: a) External nitrate concentrations. b) Loss rate derived from the data of Sjøtun (1993).

For phytoplankton it was assumed that 50% of the nutrients associated with lost biomass were instantaneously regenerated and returned to the external nutrient pool for reuse. For kelp it was assumed that the nutrients were less readily returned and 25% of nutrients due to frond loss were recycled back into the water column. There is little data at the moment to verify this number and it will depend also on the local conditions.

The model temperature was set to match those measured by Sjøtun (1993). Light conditions were not measured by Sjøtun (1993) so conditions were set based on the known latitude (60^{o} 15' N) and water depth (5m) leaving the water column light attenuation coefficient as a free parameter. This was set to a low value of 0.07 m^{-1} giving little light attenuation in the water column and was a value used by Broch & Slagstad (2011) for their simulations. Kelp was assumed to lie at 5m depth as reported in Sjøtun (1993). However the local water depth was set to 10m representing the average depth in the region surrounding the kelp beds although this number is not reported in the field study. There is a general

difficulty in calibrating the macroalgal sub-model with the nutrient and phytoplankton dynamics (including nutrient recycling) coupled in as the biomass is dependent on the available nutrient pool for example and in a coupled model this is determined by a number of factors including assumption about the local water depth and nutrient renewal rates that are not measured or reported.

The plants studied by Sjøtun (1993) had an average length of about 85cm in midwinter. Assuming the average width of the material at this point was toward the lower range of reported widths at 30cm, an estimate of area in January was obtained as 26 dm^2. To compare the area measured for individual plants with the model values it was assumed that 1 plant per square meter was grown so that the model area variable (units $dm^2\ m^{-2}$) was directly comparable with plant specific values report by Sjøtun (1993). Thus the simulation was started from the beginning of January with the initial model frond area set to 26 $dm^2\ m^{-2}$.

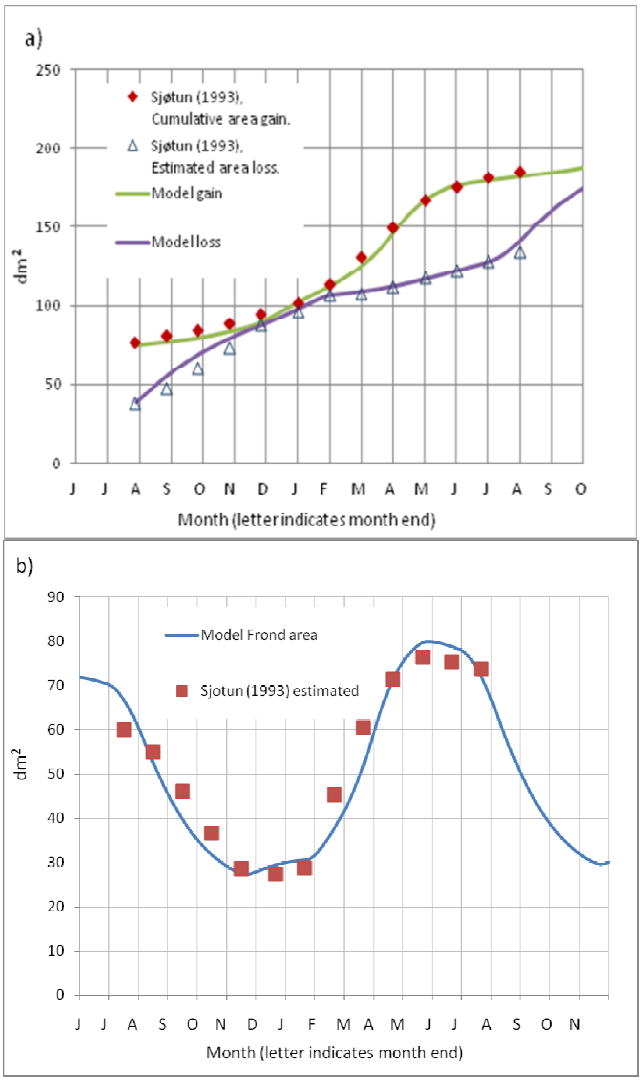

Figure 27: a) Cumulative area gain and loss compared to a reanalysis of the data of Sjøtun (1993). b) Net change in area over a growing season.

The model growth and loss rates were calibrated to match the cumulative area growth and loss estimated from the data of Sjøtun (1993). A key calibration parameter was found to be the loss rate. The re-analysis of the Sjøtun data for gain and loss of area suggest a strong seasonal variation with low rates during the peak growing period from March to the end of July and a higher loss rate from August through to February (Figure 26b). To calibrate the model, loss and growth rates were adjusted to match the observed values. The resulting cumulative area gained and lost in the model is plotted against that estimated from the Sjøtun (1993) data (Figure 27a), with the resulting net seasonal change in area is shown in Figure 27b.

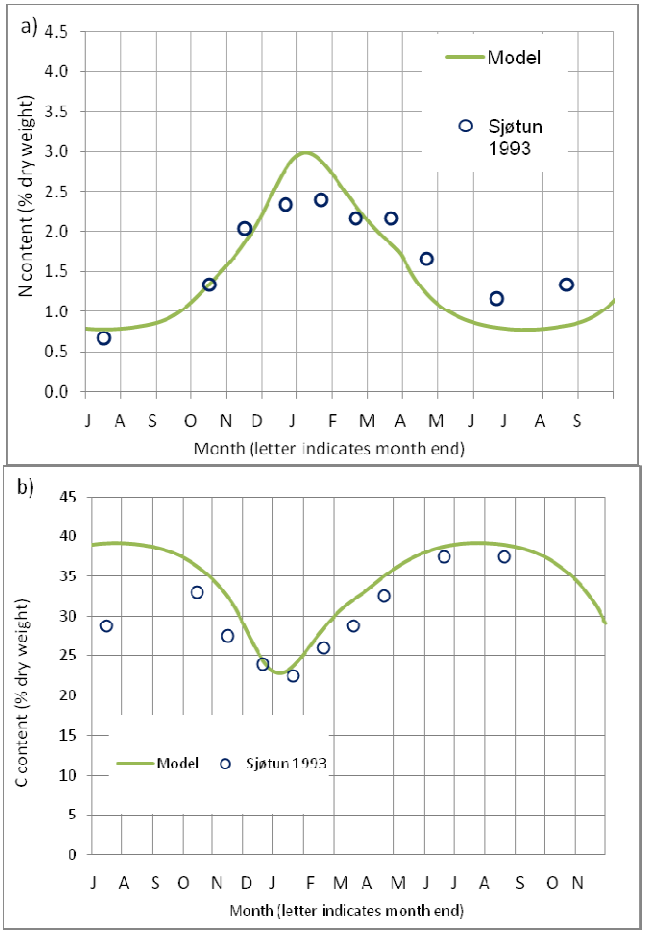

Figure 28: a) Internal nitrogen, b) internal carbon compared to the data of Sjøtun (1993)

Parameters associated with internal carbon and nitrogen content (C_{min}, N_{min}, N_{max}, respiration rate constant R_0 and exudation rate γ) were adjusted to fit the data of Sjøtun (1993). The resulting fit (Figure 28a,b) shows some differences in detail, notably the shape of the internal nitrogen curve that is more peaked than suggested by the data points and possibly a too rapid build up of stored carbon in spring. However, the results show reasonable agreement in overall behaviour and magnitude and are very similar to that reported in Broch & Slagstad (2011).

The final set of parameter values arrived at from measurements reported in the literature together with calibration with the data of Sjøtun (1993) are shown in Table 9.

Parameter description	Symbol	Value	Units	Notes
Frond area maximum growth rate	μ_{max}	0.036	d^{-1}	Calibration with Sjøtun (1993) data. Value similar to Broch & Slagstad (2011) value for larger plants.
Frond area loss rate	λ	0.01(Aug-Feb) 0.002 (Mar-July)	d^{-1}	Sjøtun (1993) data with re-analysis
Nitrogen uptake rate	V_{max}	0.2	mmol N dm^{-2} d^{-1}	From Gordillo et al. (2006) and converted from dry weight to area using conversion 0.6 g dm^{-2}
Half-saturation constant for uptake of external nitrogen	k_N	4	mmol m^{-3}	Espinoza & Chapman (1983) & Broch & Slagstad (2011).
Minimum nitrogen content (structural N only).	Q_{min}	1.1	mmol N dm^{-2}	Model calibration with data of Sjøtun (1993)
Maximum nitrogen content (structural N + full reserve)	Q_{max}	1.7	mmol N dm^{-2}	Model calibration with data of Sjøtun (1993)
C Minimum (structural C only).	C_{min}	0.11	g C dm^{-2}	Derived from Broch & Slagstad (2011) and calibration with Sjøtun (1993) data.
Exudation parameter	γ	1.5	g C dm^{-2}	Model calibration with data of Sjøtun (1993)

Table 8: Calibrated values for kelp sub- model parameters.

Photosynthetic efficiency	α	9.0 x10^{-4}	g C dm^{-2} d^{-1} (umol photons m^{-2} s^{-1})$^{-1}$	Broch & Slagstad (2011) and Luning 1979,1990)
Light saturation constant	I_k	50	umol photons m^{-2} s^{-1})$^{-}$	Lüning (1979), Drew (1983)
Respiration constant	R_0	9.0 x10^{-3}	g C dm^{-2} d^{-1} (umol photons m^{-2} s^{-1})$^{-1}$	Calibration
Respiration adjustment parameter	k_R	3.0 x10^{-3}	g C dm^{-2}	Calibration
Minimum area adjustment parameter.	δA	0.01 A_0	dm^{-2}	
Structural weight per area	k_A	0.6	g dm^{-2}	Broch & Slagstad (2011)
Conversion factor from internal carbon content to partial dry weight	k_C	2.1	g dw (g C)$^{-1}$	Broch & Slagstad (2011)
Conversion factor from internal nitrogen content to partial dry weight	k_N	0.038	g dw (mmol N)$^{-1}$	Derived from Broch & Slagstad (2011)
Percent of nutrients recycled from lost material	e_A	50	%	Fixed value

Table 9: *Continued*.

8.8 Calibration of phytoplankton sub-model

To verify that the phytoplankton component of the model is able to simulate a reasonable seasonal cycle of phytoplankton a comparison with measurements from Loch Creran on the west coast of Scotland was used. The main calibration parameter used was the heterotroph ratio. This quantity strongly influences the timing of the spring bloom. Other values were set to default values based on simulations reported for Loch Creran (Tett et al. 2003; Tett et al 2011). It should be noted that the simulations reported by Tett et al. were for a more complex two species (Diatom plus Flagellate) version of the phytoplankton

model. Here we use a single phytoplankton species set to yield a spring bloom characteristic of diatoms (however without silicon limitation being included). Phytoplankton parameters are shown in Table 10.

Parameter description	**Symbol**	**Value**	**Units**
Maximum growth rate	μ_{max}	2.37	d^{-1}
Loss rate	L	0.1	d^{-1}
Light saturation	I_k	100	umol photons m^{-2} $s^{-1})^{-}$
Half-saturation constant for uptake of external nitrogen	k_N	2	mmol m^{-3}
Heterotrophs ratio	η	25	%

Table 10: Phytoplankton parameters

9 Appendix B: implementation of nutrient sink in ERSEM-BFM

A nutrient sink was implemented in ERSEM-BFM that mimics the nutrient uptake capacity of macroalgae in a similar way as formulated for the compartment model (**Error! Reference source not found.**). The nutrients were removed completely from the model, equivalent with the assumption that there is no mortality or decay from macroalgae, and all macroalgae are harvested. The rate of nutrient removal [*mmol nutrient* m^{-3} day^{-1}] was formulated as

$$U = V_{\max} \times A \times f(N) / \Delta z$$

with V_{max} =[*mmol nutrient* dm^{-2} day^{-1}] the maximum uptake rate, one each for nitrate, ammonium, phosphate (laboratory derived), A = [dm^2 m^{-2}] macroalgae frond area per surface area of domain (A=100 is complete coverage), Δz the layer thickness occupied by the farm, and

$$f(N) = N /(N + K_N)$$

a nutrient uptake function, depending on the nutrient concentration. For this function, K_N = *mmol* m^{-3} is a half-saturation constant, one each for nitrate, ammonium, phosphate (laboratory derived). Values for V_{max} and K_N for nitrate, phosphate and ammonium are given in Table 11.

Quantity	Value	Unit
Nitrate V_{max}	2.4e-1	*mmol N* dm^{-2} day^{-1}
Nitrate K_N	4.0	*mmol N* m^{-3}
Ammonium V_{max}	2.4e-1	*mmol N* dm^{-2} day^{-1}
Ammonium K_N	4.0	*mmol N* m^{-3}
Phosphate V_{max}	2.4e-2	*mmol P* dm^{-2} day^{-1}
hosphate K_N	4.0	*mmol P* m^{-3}

Table 11. Nominal values for maximum uptake rate and half-saturation constant.

10 Appendix C: ERSEM-BFM model results

10.1 Reference scenario

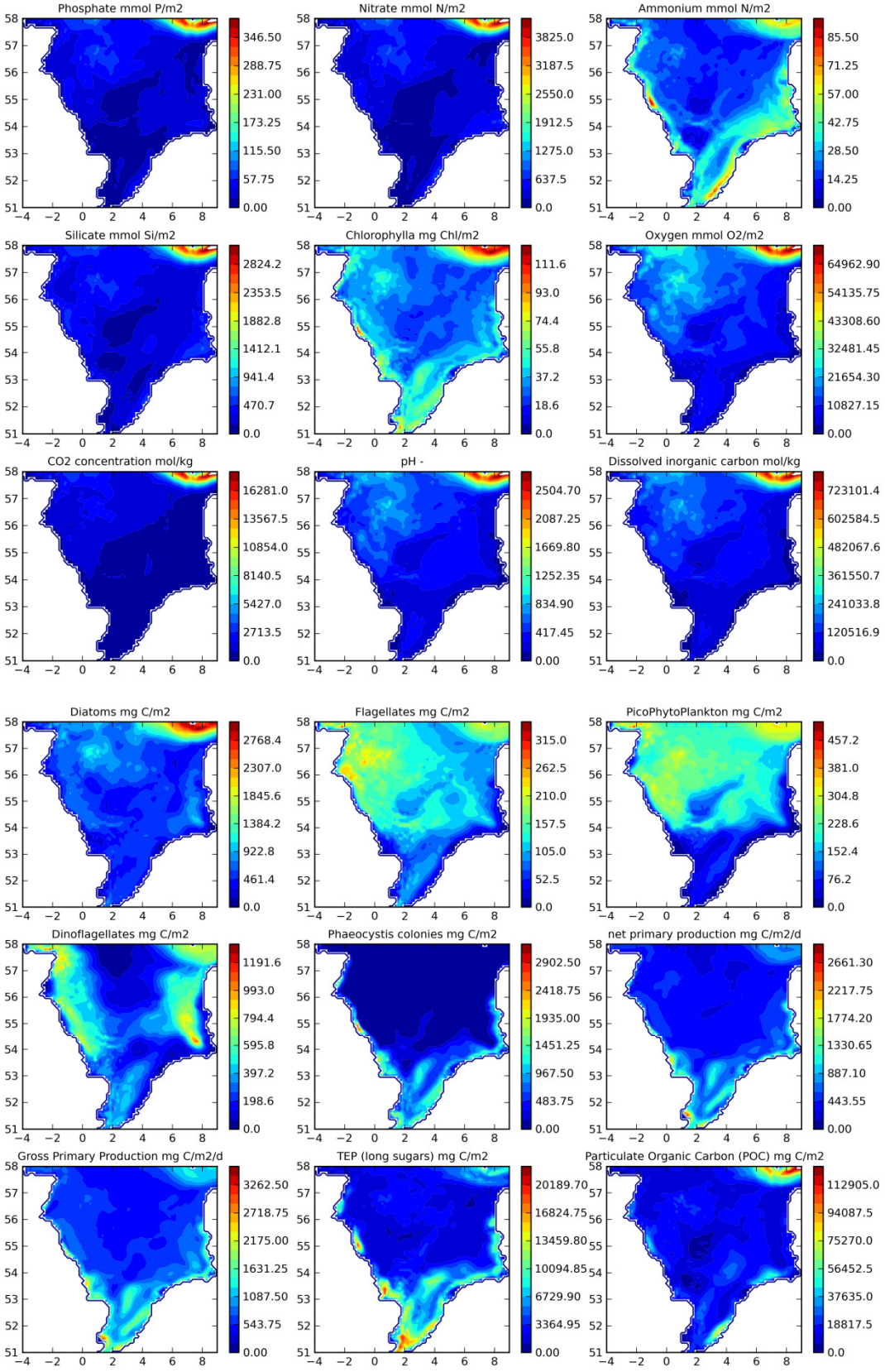

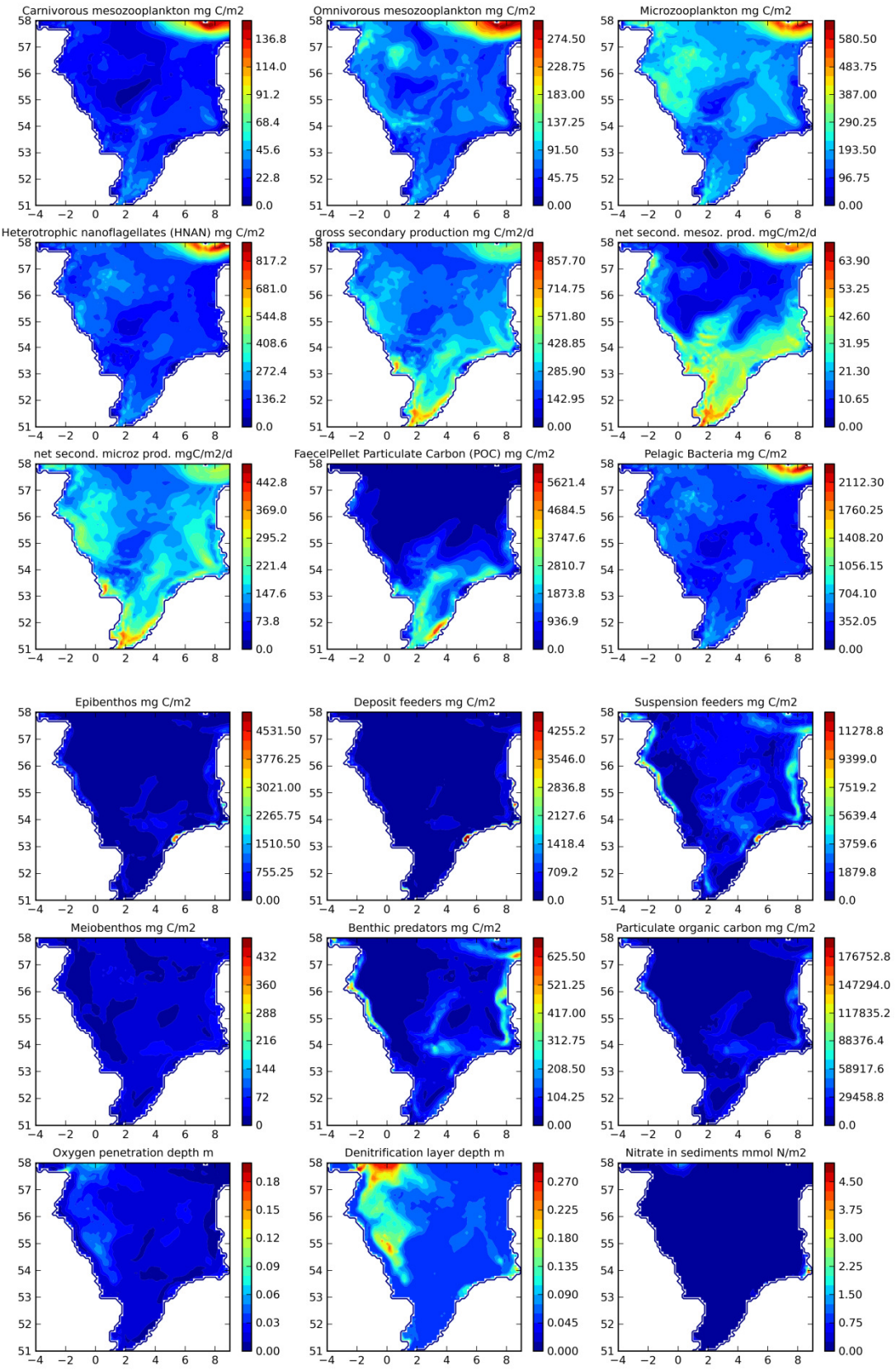

All variables were depth-integrated, annual averaged, and then averaged over 2005-2008.

10.2 Scenario 1

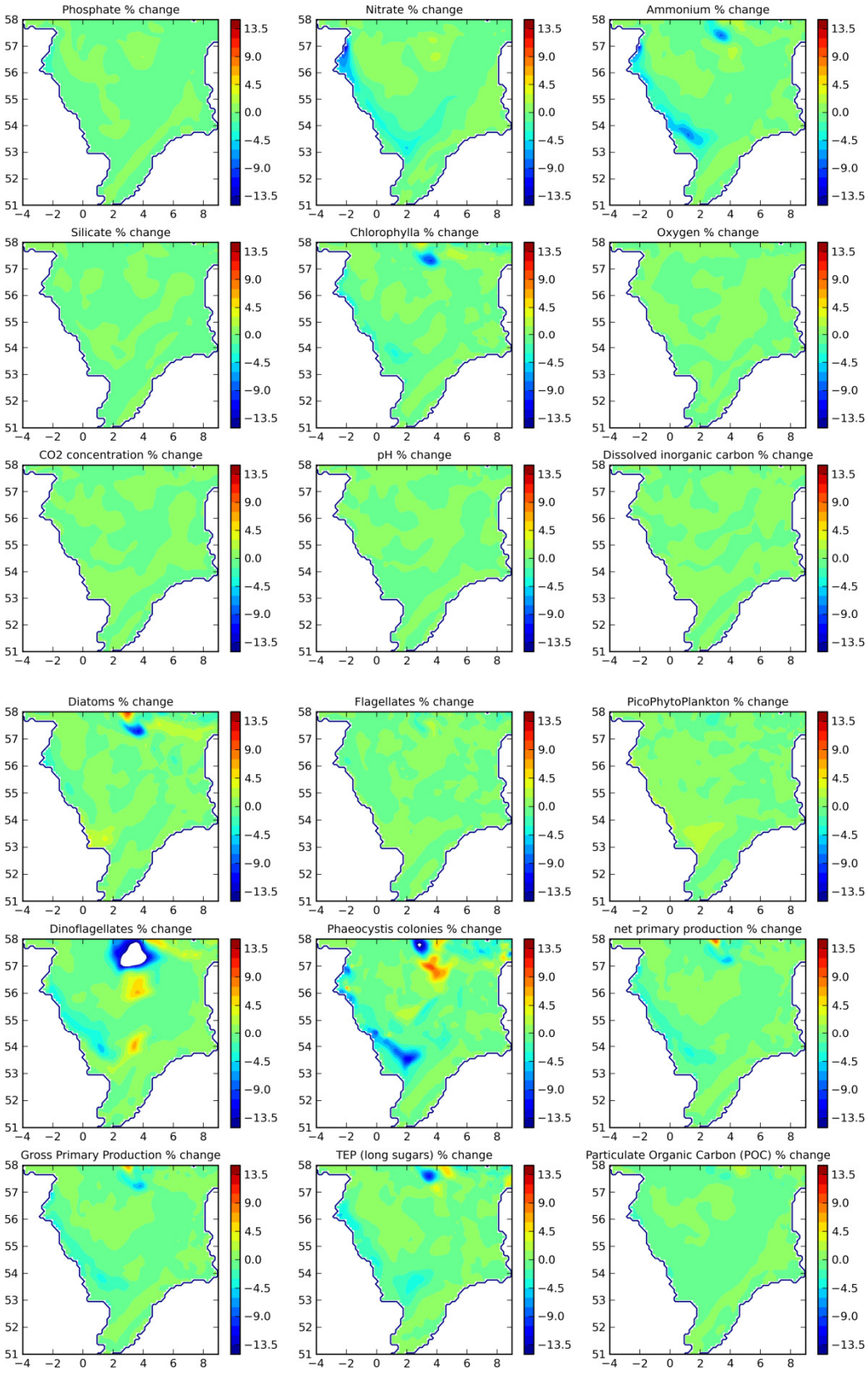

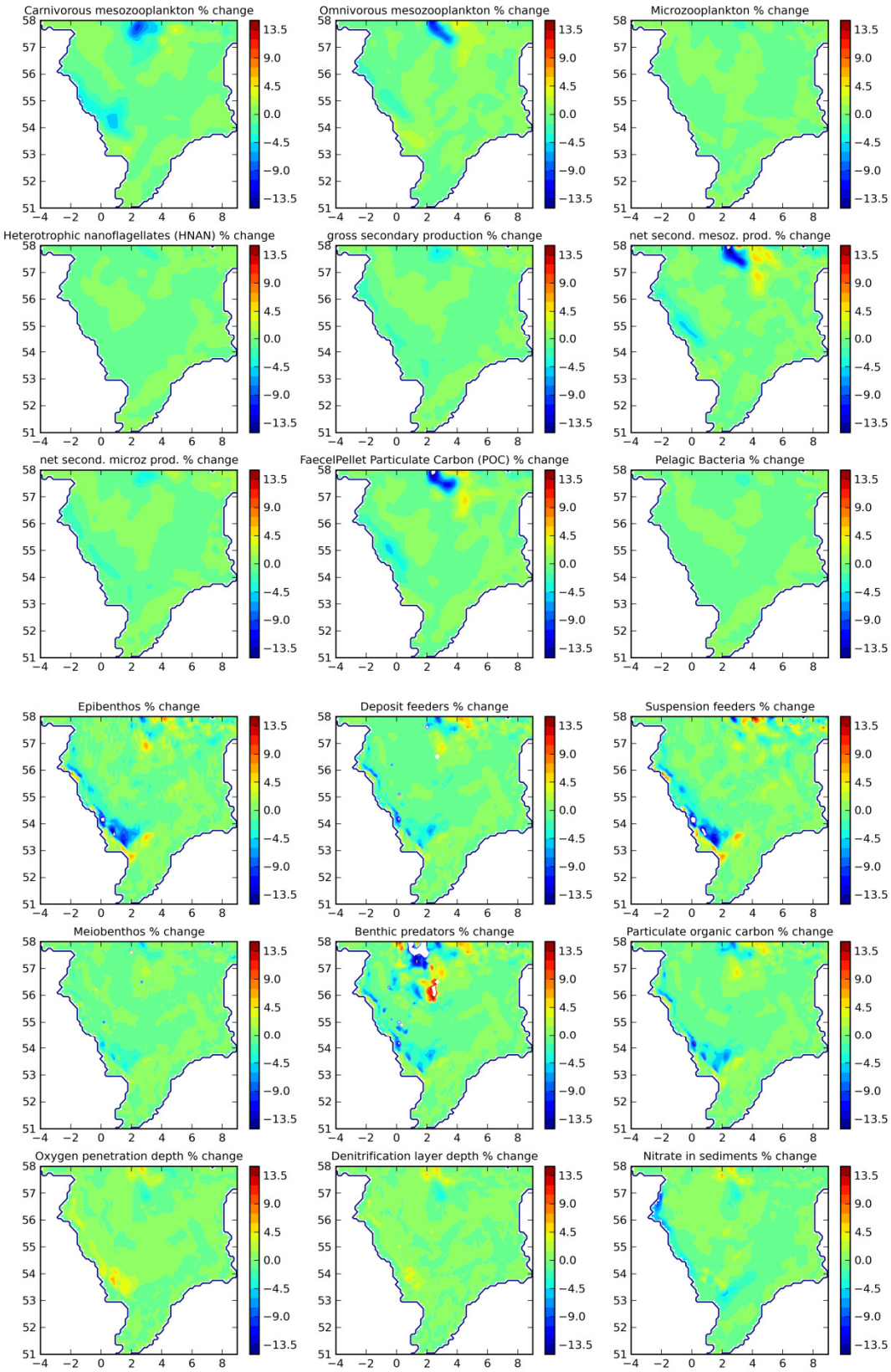

All variables were depth-integrated, annual averaged, relative difference taken, and then averaged over 2005-2008.

10.3 Scenario 4

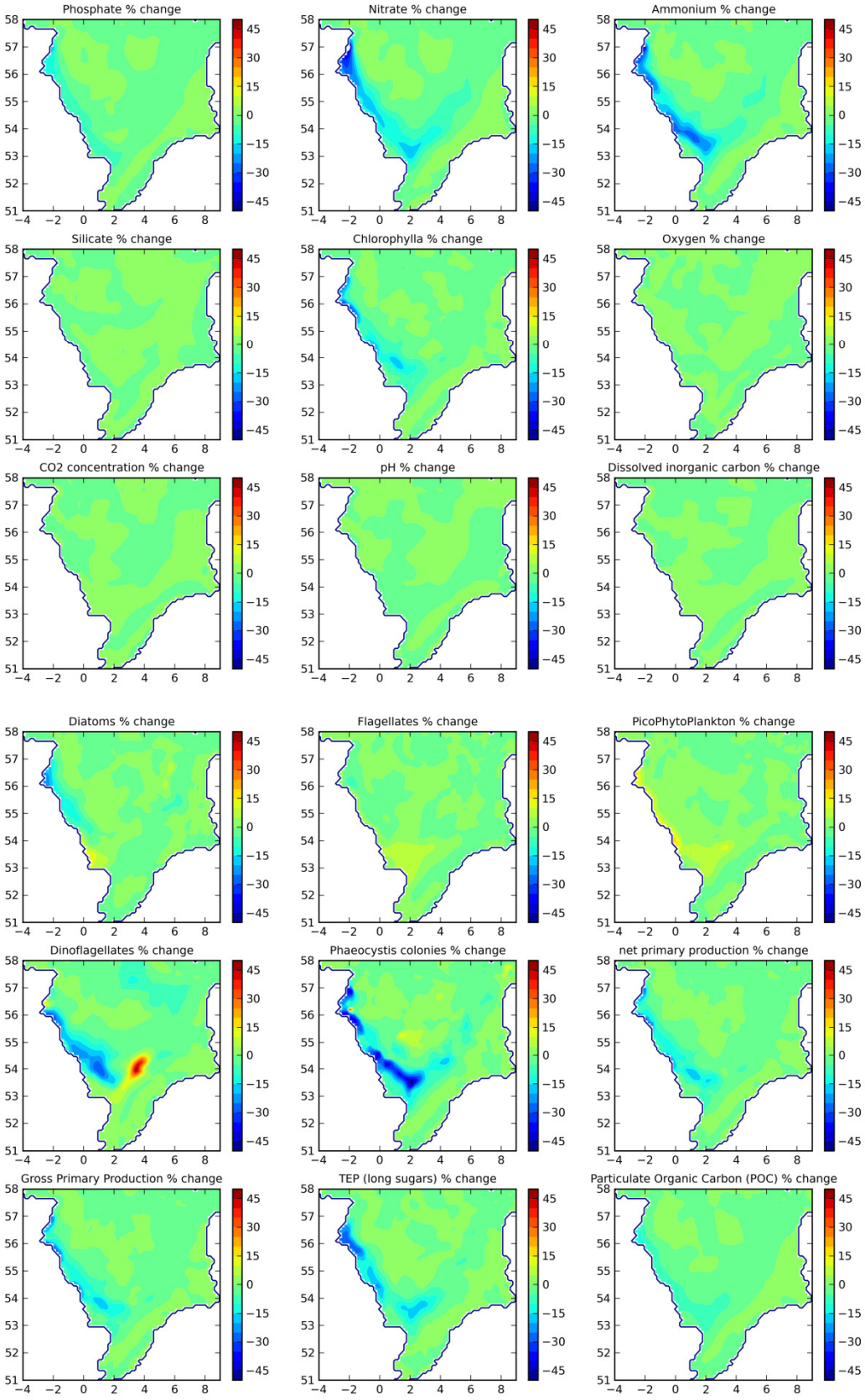

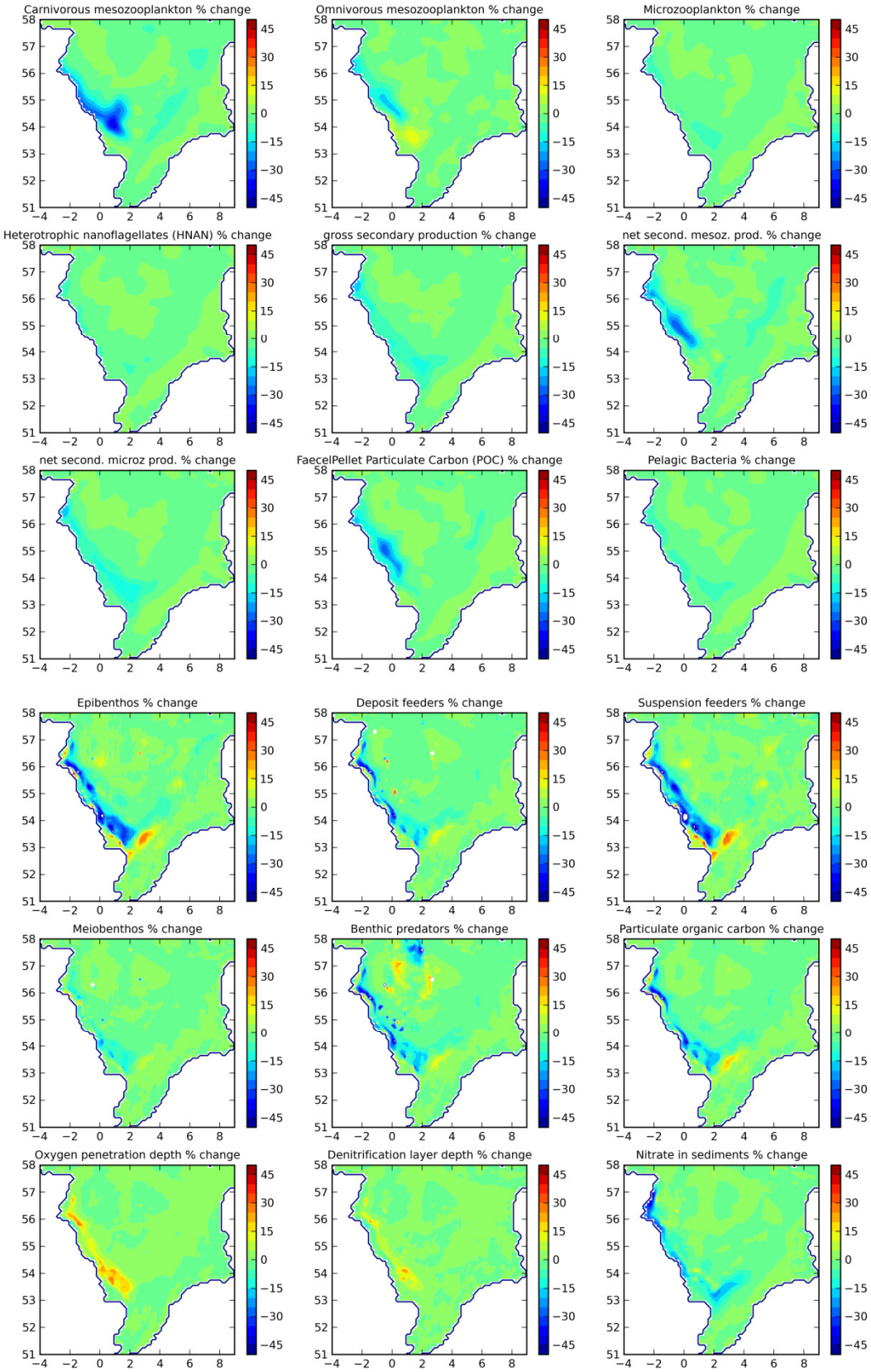

All variables were depth-integrated, annual averaged, relative difference taken, and then averaged over 2005-2008.

The Crown Estate
16 New Burlington Place
London W1S 2HX
Tel: 020 7851 5080

www.thecrownestate.co.uk

ISBN: 978-1-906410-38-4